ACS OMEGA

http://pubs.acs.org/journal/acsodf

Article

# Electrochemical Detection of Dihydroxybenzene Isomers at a Pencil Graphite Based Electrode

Md. Muzahedul I. Khan, Mohammad A. Yousuf, Parbhej Ahamed, Mohammad Alauddin, and Nusrat T. Tonu*

Cite This: *ACS Omega* 2022, 7, 29391−29405

Read Online

ACCESS | Metrics & More | Article Recommendations | Supporting Information

**ABSTRACT:** In this work, an HB pencil electrode (HBPE) was electrochemically modified by amino acids (AAs) glycine (GLY) and aspartic acid (ASA) and designated as GLY-HB and ASA-HB electrodes. They were used in the detection of dihydroxybenzene isomers (DHBIs) such as hydroquinone (HQ), catechol (CC), and resorcinol (RS), by cyclic voltammetry (CV), and by differential pulse voltammetry. HBPE was characterized by scanning electron microscopy and energy-dispersive X-ray spectroscopy. These three electrodes showed a linear relationship of current with concentration of DHBIs, and the electrochemical processes were diffusion controlled in all cases. In simultaneous detection, the limit of detection, based on signal-to-noise ratio (S/N = 3), for HQ, CC, and RS was 12.473, 16.132, and 25.25 $\mu$M, respectively, at bare HBPE; 5.498, 7.119, and 14.794 $\mu$M, respectively, at GLY-HB; and 22.459, 25.478, and 38.303 $\mu$M, respectively, at ASA-HB. The sensitivity for HQ, CC, and RS was 470.481, 363.781, and 232.416 $\mu$A/mM/cm$^2$, respectively, at bare HBPE; 364.785, 282.712, and 135.560 $\mu$A/mM/cm$^2$, respectively, at GLY-HB; and 374.483, 330.108, and 219.574, respectively, at ASA-HB. The interference studies clarified the suitability and reliability of the electrodes for the detection of HQ, CC, and RS in an environmental system. Real sample analysis was done using tap water, and the proposed electrodes expressed recovery with high reproducibility. Meanwhile, these three electrodes have excellent sensitivity and selectivity, which can be used as a promising technique for the detection of DHBIs simultaneously.

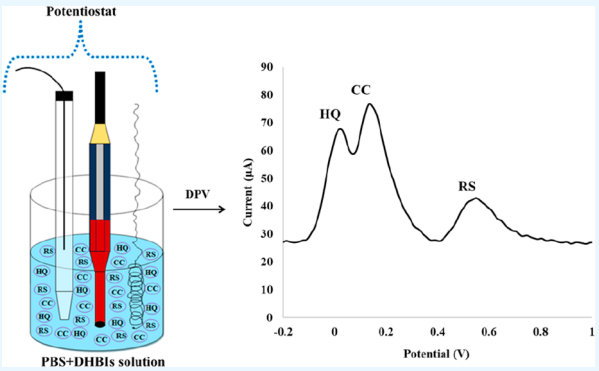


## INTRODUCTION

The evolution of science and technology is the key to the manifestations of human progress. As the saying goes, "The science of today is the technology of tomorrow". A lot of industries have been established to accomplish human desires. In doing so, many toxic chemicals are released as byproducts from these industries.[1] HQ, CC, and RS, collectively known as dihydroxybenzene isomers (DHBIs), are widely recognized as one of the most toxic environmental pollutants due to their high toxicity and low degradability in the environment.[2] They are found in the waste of many industries including paper and pulp, rubber, textiles, steel, petrochemicals, synthetic fuel conversion, dyes, plastics, pharmaceuticals, cosmetics, etc.[3] DHBIs, however, may have serious toxic consequences and lead to human health issues like pulmonary failure, a protracted rise in blood pressure, DNA damage, leukemia, skin irritation, vascular collapse, etc. due to their limited biodegradability in the ecological environment.[4] Due to their high level of exposure in the environment as well as low biodegradability, they were named potential environmental pollutants by the US Environmental Protection Agency (EPA) and European Union.[5] Hence, diverse methods which have been brought into play so far for their simultaneous detection include chromatography, fluorescence, phosphorescence, chemiluminescence, pH-based flow injection analysis, capillary electrophoretic methods, solvent extraction techniques, electrochemical methods, etc. Unlike the conventional methods, electrochemical techniques are simple, interesting, easily movable, and broadly employed.[6] Moreover, DHBIs have similar chemical structures and characteristics; they have a tendency to coexist, and the redox potentials of HQ and CC are close beside one another and practically overlap at many electrodes. Therefore, it challenging to detect them by electrochemical techniques simultaneously.[7]

To overcome these defects, numerous efforts have been made to investigate new electrode materials capable of detecting HQ, CC, and RS simultaneously, which include

Received: June 11, 2022
Accepted: August 2, 2022
Published: August 11, 2022

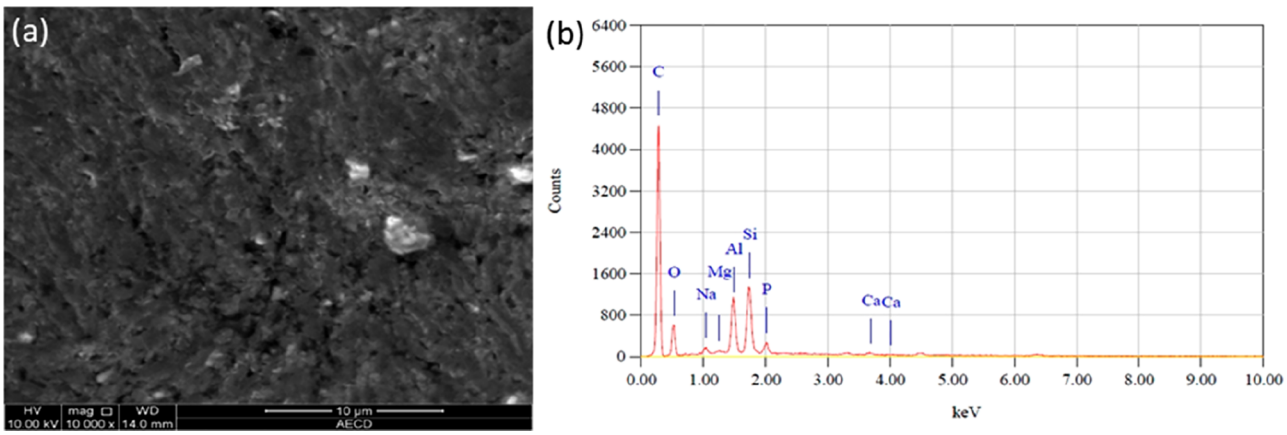


**Figure 1.** (a) SEM and (b) EDX of HBPE.

glassy carbon electrode (GCE) modified with allura red polymeric film,[1] multiwalled carbon nanotubes (MWCNTs),[8] MWCNTs/poly(1,5-diaminonaphthalene) composite film,[4] MWCNTs/ionic liquid (IL) gel,[9] Au nanoparticles (NPs) loaded on poly-3-amino-5-mercapto-1,2,4-triazole-MWCNTs film,[10] AuNPs/sulfonated grapheme,[11] poly amidosulfonic acid/MWCNTs,[12] reduced graphene oxide/magnetite NPs/AuNPs composite,[13] graphene−chitosan composite film,[14] poly(1,5-diaminonaphthalene),[15] aspartic acid,[16] tyrosinase immobilization with ordered mesoporous C−Au/L-lycine membrane/Au NPs,[17] 3D-flower-like copper sulfide nanoflake-decorated carbon nanofragments,[18] activated phosphate buffer solution (PBS),[19] MWCNT/AgNPs,[20] polyglutamic acid,[21] 2-(phenylazo) chromotropic acid-(CH−) conducting polymer,[22] electrochemically reduced grapheme oxide-poly-(Eriochrome black T)/Au NPs,[23] poly(*p*-aminobenzoic acid),[24] tyrosinase/Au NPs encapsulated-dendrimer bonded conducting polymer,[25] self-assembled $Ti_3C_2$/MWCNTs nanocomposites,[26] C/Au nanostructured materials,[27] graphene oxide/polymelamine composite,[28] carbon nanocoils/zinc-tetraphenylporphyrin nanocomposite,[6] nitrogen doped porous carbon nanopolyhedrons-MWCNTs hybrid materials,[29] thionine/graphene oxide,[30] gel of 1-butyl-3-methylimidazolium hexafluorophosphate (BMIHP)/MWCNTs,[31] ammonium carbamate,[32] poly(malachite green)/MWCNT film,[33] carboxy-functionalized CNTs/chitosan matrix/Au Nps,[34] Pd NPs/poly(1,5-diaminonaphthalene) matrix;[35] pencil graphite electrode (PGE) modified with CNTs,[5] BIHP,[2] poly(direct yellow 11),[36] cobalt-phthalocyanine;[37] mesoporous Pd electrode,[38] poly(crystal violet);[39] flexible screen printed carbon electrode;[40] graphene sheets embedded carbon films;[41] poly-(adenine)/graphene paste electrode;[3] carbon ionic liquid electrode modified with graphene,[42] Au NPs/graphene;[43] gold electrode modified with gold atomic cluster-poly(3,4-ethylenedioxidethiophene) nanocomposite,[44] etc. However, it remains challenging to investigate novel electrode materials for simultaneous detection of DHBIs with a wide linear range and higher sensitivity.

In recent times, PGE and carbon paste electrode (CPE) have been fabricated rapidly for their outstanding performance.[51] CPEs are composed of only carbon or an organic binder such as Nujol, silicone oil, paraffin oil, ionic liquids, etc. and express themselves as a custom-made electrode for users, where PGE is a solid rod of graphite obtained from a lead pencil. Depending on users preferences, the composition of the paste of CPE could be easily varied by changing the ratio of carbon dust and binder, and the purity of CPE could be maintained by maintaining the purity of carbon dust and binder as much as possible at 100%. However, as an industrially produced graphite rod, its properties could not be varied.[49] According to the European letter scale, pencil leads are labeled with letters 9H (the hardest) to 8B (the softest). B type pencil lead contains more graphite and H type has more binder.[50] Unlike CPE, PGE could be easily purchased from a local stationary shop. Specialization is needed to fabricate and handle CPE, whereas PGE can be easily fabricated and is easy to handle. Both CPE and PGE have a small renewable surface area and provide a high signal-to-noise ratio and short response time for small amounts of sample.[45]

Countless applications have been developed based on PGE sensors, such as detection of antioxidants and biological compounds,[46] DNA hybridization related to *Microcystis* spp.,[47] ascorbic acid,[48] paracetamol,[45] etc., as well as the detection of DHBIs.[5,2,36,37]

Recently, PGE has been successfully used to fabricate several biosensors because of its high electrochemical reactivity, conductivity, mechanical rigidity, ease of modification, low background current, and low cost.[45] Amino acids (AAs) have engrossed much consideration for their superior physical and chemical features. Besides they have much more inimitable lead for biosensor fabrication instead of conventional modification chemicals.[2] To the best of our knowledge, the simultaneous detection of DHBIs at poly- GLY and poly-ASA modified PGE has not been reported yet. In this study, HBPE was modified electrochemically by GLY and ASA. HBPE, GLY-HB, and ASA-HB electrodes were used in the detection of DHBIs by CV and DPV.

## RESULTS AND DISCUSSION

**Surface Features of HBPE.** Figure 1a shows the SEM image of bare HBPE. Grayish black color indicates graphite on the surface of bare HBPE. The surface is uneven and contains many pits and trenches. White spots of different sizes are present discretely on its surface. Figure 1b shows the EDX values of the bare HBPE surface. It is composed of 74.91% carbon, 9.84% Si, 7.38% Al, 4.63% $O_2$, 1.89% P, and trace amounts of Na, Ca, and Mg.

The internal structure and composition of an electrode can determine the rate of the electron-transfer process. Sometimes



https://doi.org/10.1021/acsomega.2c03651
ACS Omega 2022, 7, 29391−29405

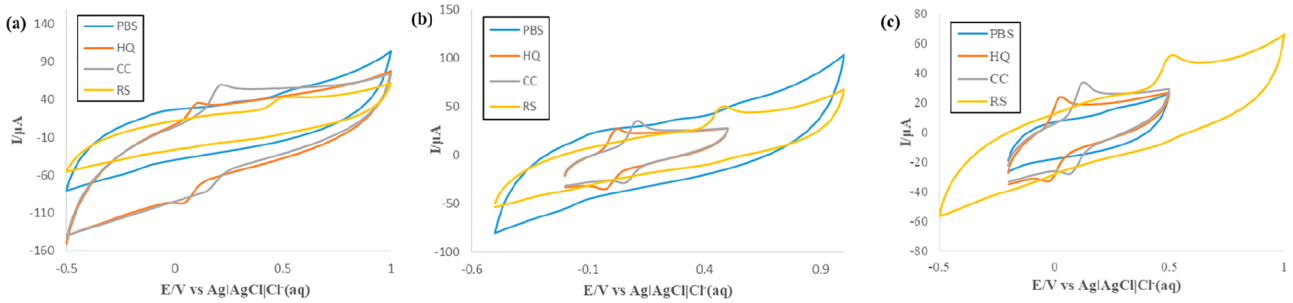


**Figure 2.** CVs of 1 mM HQ, CC and RS in PBS at 50 $mVs^{-1}$ on bare (a) HBPE, (b) GLY-HB, and (c) ASA-HB.

the electrochemical activity of an electrode toward redox probes could be increased by manually controlling the types and densities of surface defects, especially for a 2D electrode. Defects can not only regulate or/and alter the composition of an electrode but also improve the electrochemical performance. Sometimes defects could increase the electrocatalytic activity of the carbon atom. The analyses from SEM and EDX indicate that HBPE is mainly graphite composite material, its lead is not pure graphite and it has a lot of vacancies, point defects, and foreign materials. Because PGE was fabricated from locally available wooden pencils, its defects and vacancies could not be controlled manually. Having a renewable surface, its defects and vacancies could affect the electrochemical activities of HBPE toward DHBIs. Thus, the properties of new surfaces of GLY-HB and ASA-HB would also be affected by these vacancies and defects, thereby changing their electrochemical activities.[52−54]

**Effect of pH.** The electrochemical behavior of DHBIs at bare HBPE, GLY-HB, and ASA-HB electrodes were studied using CV over the pH range 3−11. pH was controlled by the addition of acetate buffer (pH 3−5), phosphate buffer (pH 6−8), and carbonate buffer (pH 9−11) solutions as supporting electrolytes. The anodic peak currents of DHBIs increased slowly with a rise in pH from untilo 6.8 in all cases and then decreased toward the three electrodes under investigation. Therefore, pH 6.8 was considered as the optimum pH, and the whole experiment was carried out in pH 6.8.

**Cyclic Voltammetry Behavior of DHBIs in PBS at Bare HBPE, GLY-HB, and ASA-HB.** Figure 2 shows the CVs of 1 mM HQ, CC, and RS in PBS at 50 $mVs^{-1}$ on bare (a) HBPE, (b) GLY-HB, and (c) ASA-HB electrodes. In all cases, there was no peak for PBS. After addition of HQ or CC or RS in PBS at HBPE, GLY-HB, and ASA-HB, HQ gave anodic (+0.11 V, 17.87 μA; 0.026 V, 20.16 μA; +0.03 V, 13.03 μA) and cathodic peaks (+0.034 V, 15.66 μA; −0.034 V, 19.12 μA; −0.028 V, 12.05 μA), respectively; CC gave anodic (+0.216 V, 21.12 μA; +0.112 V, 31.46 μA; +0.132 V, 13.29 μA) and cathodic peaks (+0.13 V, 17.02 μA; +0.048 V, 22.83 μA; +0.06 V, 6.73 μA), respectively; and RS gave only anodic peaks (+0.53 V, 16.22 μA; +0.484 V, 17.38 μA; +0.514 V, 14.78 μA), respectively.

At the surface of the three electrodes, the ratio of anodic and cathodic peak currents of HQ is almost unity; i.e., all the HQ molecules were electroactive and gave a reduction peak after oxidation. That for CC is more than unity; i.e., some of the CC molecules gave stable products, leaving a portion of molecules that were electroactive and gave reduction peaks. So, HQ gave electrochemically reversible and CC gave electrochemically quasi-reversible redox reactions. RS gave only an oxidation peak and no reduction peak and indicated electrochemically irreversible redox reactions indicating that all the RS molecules gave stable products after oxidation.

From Figure 2, it is also seen that the CVs are tilted. This is because the PGE is not a sintered electrode at all and also may be due to the lack of purging of the solution by inert gas. Being commercially available, the surface defects and vacancies of PGE cannot be controlled manually, and being nonsintered, a reference electrode causes nonuniform distribution of current in the solution. If it was possible to sinter PGE, the surface became less defected and the crystal structure was more closely packed with active materials.[55−58]

**Effect of Scan Rates for HQ-PBS, CC-PBS, and RS-PBS system.** In PBS (pH 6.8), at different scan rates, CVs of 5 mM HQ at bare HBPE (Figure S1a) and 1 mM HQ at GLY-HB (Figure S1b) and ASA-HB (Figure S1c); 5 mM CC at bare HBPE (Figure S3a) and 1 mM CC at GLY-HB (Figure S3b, and ASA-HB (Figure S3c); 5 mM RS at bare HBPE (Figure S5a) and 1 mM RS at GLY-HB (Figure S5b) and ASA-HB (Figure S5c) were taken. It was seen that with the increasing scan rate, anodic (HQ, CC, and RS) and cathodic (HQ and CC) peak currents increased and anodic peaks (HQ, CC, and RS) shifted toward positive potential and those of cathodic peaks(HQ and CC) toward negative potential, resulting in an increase in peak potential separation (HQ and CC). It is indicated that there is a limitation for the charge-transfer kinetics or ohmic potential (*iR* drop). The passage of current through the cell requires a potential or driving force to overcome the resistance of ions to move toward the electrode, referred as *iR* drop. The peak current of anodic and/or cathodic peaks increased with increasing square root of scan rate (Figure S1d−f, Figure S3d−f, and Figure S5d−f); the corresponding trend line almost passed through the origin, indicating the processes were diffusion controlled.

**Effect of Concentration for HQ-PBS, CC-PBS, and RS-PBS Systems.** In PBS (pH 6.8), at a scan rate of 0.05 V $s^{-1}$ and at different concentrations, CVs of HQ at bare HBPE (Figure S2a), GLY-HB (Figure S2b), and ASA-HB (Figure S2c), CC at bare HBPE (Figure S4a), GLY-HB (Figure S4b), and ASA-HB (Figure S4c), and RS at bare HBPE (Figure S6a), GLY-HB (Figure S6b), and ASA-HB (Figure S6c) were taken. The peak currents increased with increasing concentrations (Figure S2d−f, Figure S4d−f, and Figure S6d−f). All graphs gave good linearity, and the correlation coefficient values for HQ, CC, and RS were $R^2$ = 0.9999(a), $R^2$ = 0.9997(c); $R^2$ = 0.9996(a), $R^2$ = 0.9998(c), and $R^2$ = 0.9866(a) at bare HBPE; $R^2$ = 0.9977(a), $R^2$ = 0.9999(c); $R^2$ = 0.9952(a), $R^2$ = 0.9951(c), and $R^2$ = 0.9975(a) at GLY-HB; and $R^2$ = 0.998(a), $R^2$ = 0.988(c); $R^2$ = 0.9961(a), $R^2$ = 0.9856(c), and $R^2$ = 0.9986(a) at ASA-HB, respectively.



https://doi.org/10.1021/acsomega.2c03651
ACS Omega 2022, 7, 29391−29405

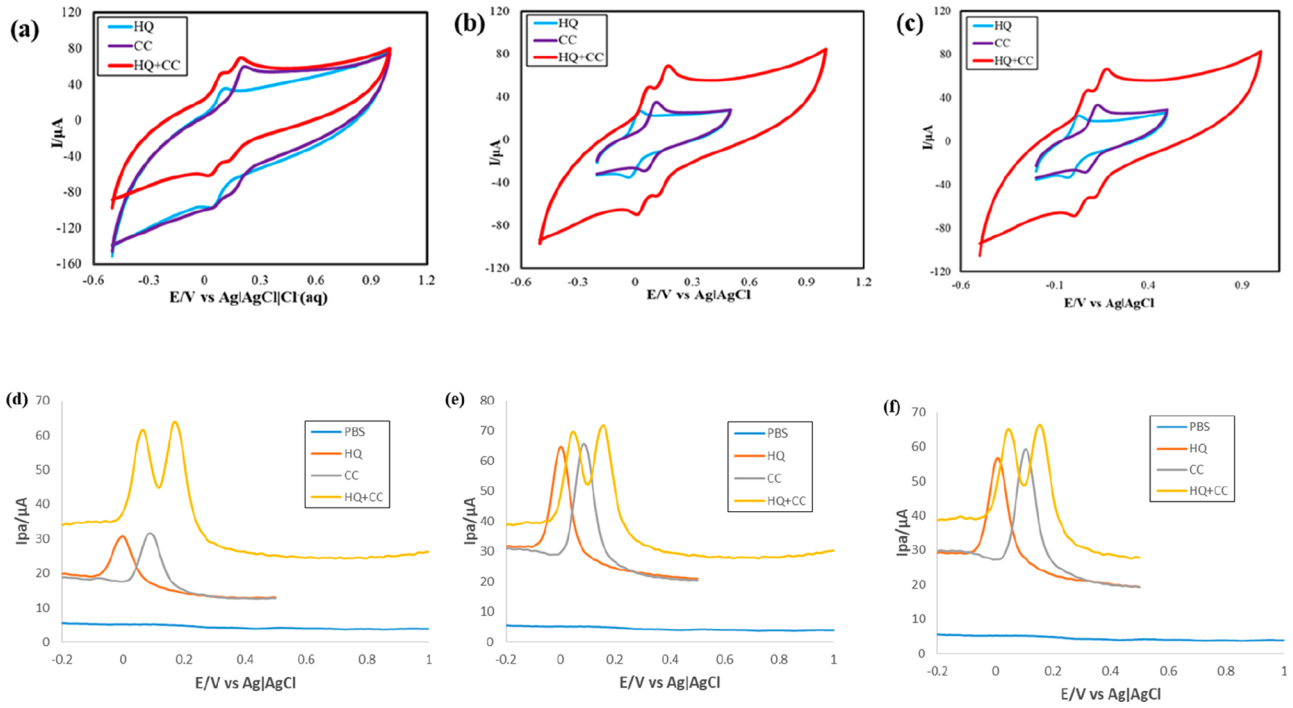


**Figure 3.** CV of 1 mM of HQ, CC and simultaneous HQ+CC in PBS at 50 $mVs^{-1}$ on (a) HBPE, (b) GLY-HB, and (c) ASA-HB. DPV of 1 mM of HQ, CC, and simultaneous HQ+CC in PBS at 50 $mVs^{-1}$ on (d) HBPE, (e) GLY-HB, and (f) ASA-HB.

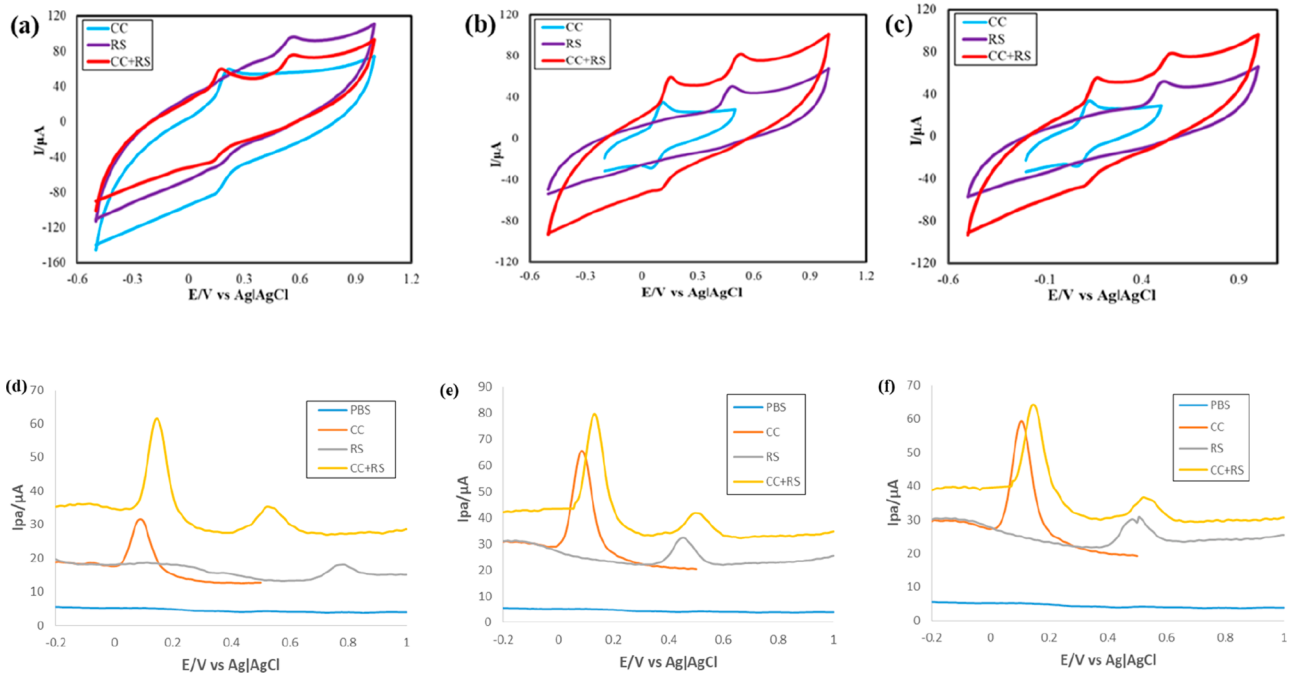


**Figure 4.** CV of 1 mM of CC, RS, and simultaneous CC+RS in PBS at 50 $mVs^{-1}$ on (a) HBPE, (b) GLY-HB, and (c) ASA-HB. DPV of 1 mM of CC, RS and simultaneous CC+RS in PBS at 50 $mVs^{-1}$ on (d) HBPE, (e) GLY-HB, and (f) ASA-HB.

**Simultaneous Detection of HQ and CC in Their Binary Mixture.** Solutions of 1 mM HQ, 1 mM CC, and a mixture of 1 mM HQ and 1 mM CC were taken in PBS (pH 6.8). CVs of single solutions as well as a binary mixture (Figure 3a) were taken at a scan rate 50 $mVs^{-1}$ at HBPE. HQ in PBS gave anodic and cathodic peaks at +0.11 V and at +0.034 V with peak currents 20.16 and 19.12 $\mu$A, respectively. On the other hand, CC in PBS gave anodic and cathodic peaks at +0.216 and +0.14 V with peak currents 31.46 and 22.83 $\mu$A, respectively. When the binary mixture of HQ and CC was investigated, two anodic peaks were found at +0.09 and at +0.198 V with peak currents of 20.7 and 27.98 $\mu$A, respectively, which are at relatively lower potentials than those for individual HQ and CC. In addition, two cathodic peaks were found at +0.016 and +0.13 V with peak currents of 14.14 and 20.76 $\mu$A, respectively, which are also at lower potentials than the peaks for individual HQ and CC. Bare HBPE could separate the anodic and cathodic peaks of HQ



https://doi.org/10.1021/acsomega.2c03651
ACS Omega 2022, 7, 29391−29405

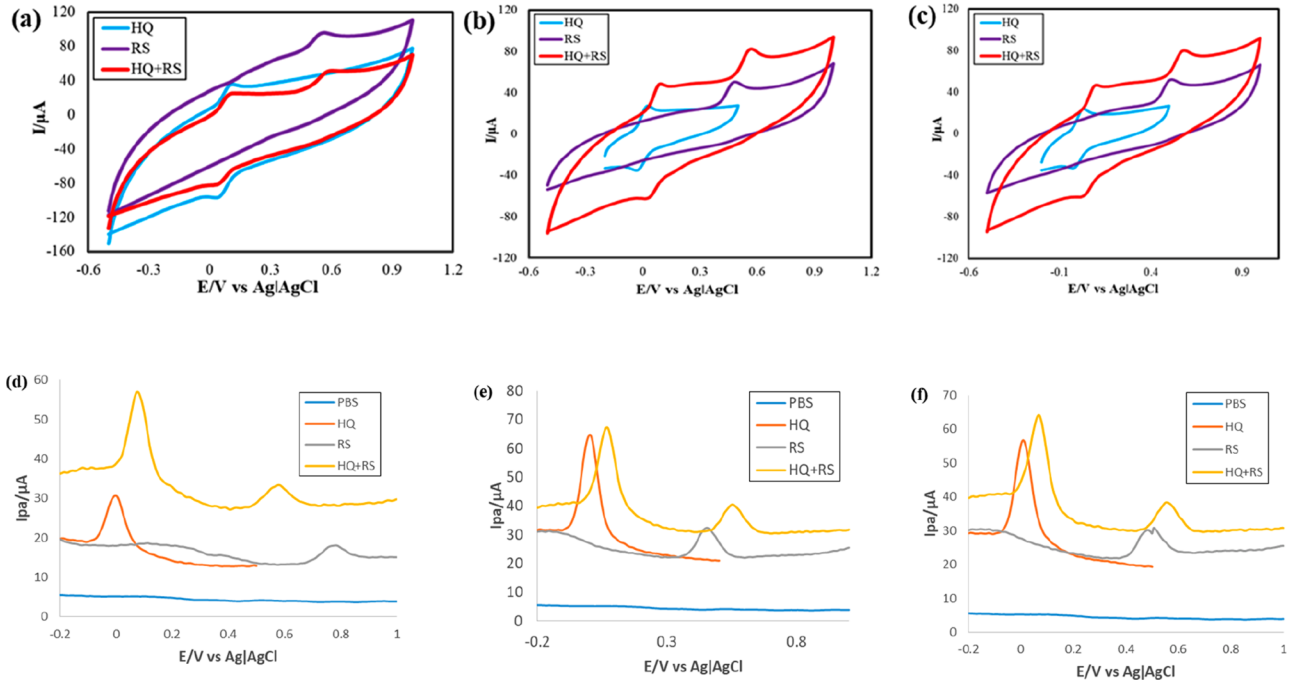


**Figure 5.** CV of 1 mM of HQ, RS and simultaneous HQ+RS in PBS at 50 $mVs^{-1}$ on (a) HBPE, (b) GLY-HB, and (c) ASA-HB. DPV of 1 mM of HQ, RS, and simultaneous HQ+RS in PBS at 50 $mVs^{-1}$ on (d) HBPE, (e) GLY-HB, and (f) ASA-HB

and CC when they are present in a binary mixture. Thus, simultaneous detection of HQ and CC from their binary mixture at bare HBPE is possible simply by CV. This separating ability of the bare HBPE can be used to detect both HQ and CC in their binary mixture, qualitatively. For quantitative estimation DPV was employed. All of the DPV experiments were taken at $E_{step}$ 0.005 V, $E_{pulse}$ = 0.02 V, and $t_{pulse}$ = 20 ms. DPVs of single solutions as well as a binary mixture (Figure 3d) were taken at a scan rate of 50 $mVs^{-1}$ at HBPE. HQ and CC give two sharp and well-defined peaks at +0.065 and +0.17 V with peak currents of 21.47 and 26.49 $\mu$A, respectively, in the binary mixture. This separating ability of bare HBPE can be used to detect both HQ and CC in their binary mixture quantitatively. CVs and DPVs of single and binary mixtures were also performed for both GLY-HB (Figure 3b,e) and ASA-HB (Figure 3c,f). At GLY-HB, by CV, HQ gave anodic and cathodic peaks at +0.026 and −0.034 V, respectively, and CC gave anodic and one cathodic peaks at +0.112 and +0.048 V, respectively. In a binary mixture, HQ and CC gave two sharp and well-defined anodic peaks at +0.068 and +0.178 V with peak currents of 26.98 and 20.9 $\mu$A, respectively, and two cathodic peaks at +0.006 and +0.116 V with peak currents of 15.7 and 13.84 $\mu$A, respectively. In DPV, HQ and CC give two sharp and well-defined peaks at +0.065 V and +0.155 V with peak current 21.38 $\mu$A and 28.86 $\mu$A, respectively. At ASA-HBPE, in CV, HQ gave anodic and cathodic peaks at +0.03 V and −0.028 V, respectively. CC gave anodic and cathodic peaks at +0.132 and +0.06 V, respectively. In a binary mixture, HQ and CC gave two sharp and well-defined anodic peaks +0.076 and +0.172 V, respectively, and two cathodic peaks at +0.012 and at +0.116 V, respectively. In DPV, HQ and CC gives sharp and well-defined peaks at +0.045 and +0.155 V, respectively, in a binary mixture. Thus, both CV and DPV can be used to detect HQ and CC in their binary mixture qualitatively at GLY-HBPE and ASA-HBPE. We can also see from the figures that in the case of DPV the peaks are sharp and clear in comparison with the CV. Thus, for quantitative determination, DPV is more favorable than CV.

**Simultaneous Detection of CC and RS in Their Binary Mixture.** Like the previous experiment, here solution of 1 mM CC, 1 mM RS and a mixture of 1 mM CC and 1 mM RS was taken in PBS (pH 6.8). CVs and DPVs of single solutions as well as binary mixture were performed at scan rate 50 $mVs^{-1}$ at HBPE (Figure 4a,d), GLY-HBPE (Figure 4b,e), and ASA-HBPE (Figure 4c,f). At HBPE in CV, CC gave anodic and cathodic peaks at +0.216 and +0.13 V with peak currents of 31.46 and 22.83 $\mu$A, respectively. On the other hand, RS gave only an anodic peak at +0.53 V with a peak current 16.22 $\mu$A. When the binary mixture of CC and RS was investigated, two anodic peaks were found at +0.178 and 0.564 V with peak currents of 25.19 and 14.98 $\mu$A, respectively. A cathodic peak for CC in the binary mixture was at +0.12 V with peak currents of 16.29 $\mu$A, which is at relatively lower potential than the individual peak for CC solution. RS gave an anodic peak with relatively higher potential than CC. In DPV, CC and RS give two sharp and well-defined peaks at +0.145 and +0.525 V with peak currents of 29.24 and 8.38 $\mu$A, respectively, and express relatively high peak potential separation for easy detection. At GLY-HBPE in CV, CC gave one anodic and one cathodic peak at +0.112 and +0.048 V, respectively. RS gave only one anodic peak at +0.484 V. In a binary mixture, CC and RS gave two sharp and well-defined anodic peaks at +0.154 and +0.532 V with peak currents of 28.43 and 19.01 $\mu$A, respectively. The cathodic peak for CC was at +0.096 V with a peak current of 15.41 $\mu$A. In DPV, CC and RS gave two sharp and well-defined peaks at +0.155 and +0.495 V having high peak separation potential with peak currents of 28.86 and 9.56 $\mu$A, respectively. At ASA-HBPE, by CV, CC gave one anodic and one cathodic peak at +0.132 and +0.06 V, respectively. RS in PBS gave only one anodic peak at +0.514 V. For the binary mixture, two sharp and well-defined anodic peaks at +0.166 and +0.552 V were found. The cathodic peak for CC in a binary mixture was



https://doi.org/10.1021/acsomega.2c03651
ACS Omega 2022, 7, 29391−29405

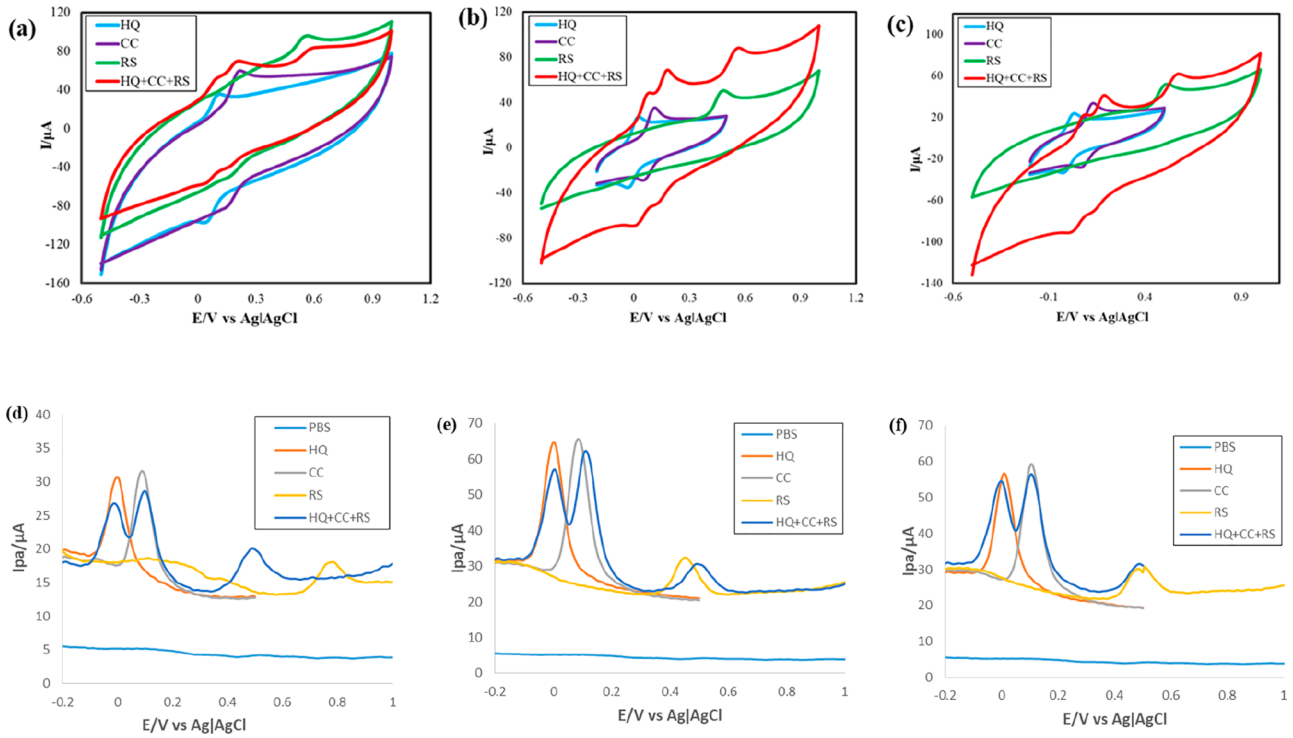


**Figure 6.** CV of 1 mM of HQ, CC, RS, and simultaneous HQ+CC+RS in PBS on (a) HBPE, (b) GLY-HB, and (c) ASA-HB at 50 $mVs^{-1}$. DPV of 1 mM of HQ, CC, RS, and simultaneous HQ+CC+RS in PBS on (d) HBPE, (e) GLY-HB, and (f) ASA-HB at 50 $mVs^{-1}$.

at +0.108 V. In DPV, CC and RS gave two sharp and well-defined peaks at +0.145 and +0.526 V, respectively, and could be useful for quantitative detection.

**Simultaneous Detection of HQ and RS in Their Binary Mixture.** Individual as well as binary mixtures of 1 mM HQ and 1 mM RS were taken in PBS (pH 6.8). CVs and DPVs were performed at HBPE (Figure 5a,d), GLY-HBPE (Figure 5b,e), and ASA-HBPE (Figure 5b,f). At HBPE, in CV, HQ gave anodic and cathodic peaks at +0.11 and +0.034 V with peak currents 20.16 and 19.12 μA, respectively. On the other hand, RS gave only an anodic peak at +0.53 V with a peak current of 16.22 μA. In a binary mixture, two anodic peaks were found at +0.12 and +0.588 V with peak currents of 21.04 and 15.42 μA, respectively, with high peak separation potential, and a cathodic peak for HQ in binary mixture was at +0.042 V with a peak current of 17.96 μA. In DPV, HQ and RS gave two sharp and well-defined peaks at +0.075 and +0.58 V with peak currents of 19.08 and 6.25 μA, respectively, at large peak separation potential, expressing the possibility of quantitative detection. At GLY-HBPE, in CV, HQ gave one anodic and one cathodic peak at +0.026 and −0.034 V, respectively. RS gave only one anodic peak at +0.484 V. For the binary mixture, HQ and RS gave two sharp and well-defined anodic peaks at +0.092 and +0.568 V with peak currents of 21.18 and 19.74 μA, respectively. The cathodic peak for HQ in the binary mixture was at +0.026 V with a peak current 17.48 μA. In DPV, HQ and RS gave two sharp and well-defined peaks at +0.065 and +0.17 V with peak currents of 20.84 and 10.08 μA, respectively, in a binary mixture, indicating affirmative conditions for quantitative detection. At ASA-HBPE, in CV, HQ gave anodic and cathodic peaks at +0.03 and −0.028 V, respectively. RS gave only an anodic peak at +0.514 V. In the binary mixture, HQ and RS gave two sharp and well-defined anodic peaks at +0.094 and +0.58 V, respectively. The cathodic peak for HQ was at +0.018 V with a peak current 17.48 μA. In DPV, HQ and RS gave two sharp and well-defined peaks at +0.07 and +0.555 V, respectively, in the binary mixture, favorable for quantitative estimation.

**Simultaneous Detection of HQ, CC, and RS in Their Ternary Mixture.** A similar solution was prepared, but ternary instead of binary as well as individual for 1 mM HQ, 1 mM CC, and 1 mM RS in PBS (pH 6.8). CVs and DPVs were performed at HBPE (Figure 6a,d), GLY-HBPE (Figure 6b,e), and ASA-HBPE (Figure 6c,f). At HBPE, in CV, HQ gave anodic and cathodic peaks at +0.11 and +0.034 V with peak currents of 20.16 and 19.12 μA, respectively. CC gave anodic and cathodic peaks at +0.216 and +0.13 V with peak currents of 31.46 and 22.83 μA, respectively. RS gave only an anodic peak at +0.53 V with peak currents of 16.22 μA. In the case of a ternary mixture, HQ, CC, and RS gave three sharp and well-defined anodic peaks at +0.09, +0.196, and +0.586 V with peak currents of 13.02, 20.38, and 11.0 0 μA, respectively. Two cathodic peaks were found at +0.044 and +0.156 V with peak currents of 12.89 and 15.02 μA for HQ and CC, respectively. In DPV, for individual solution, HQ gave a peak at 0.00 V with a peak current 14.1 μA, CC gave a peak at +0.485 V with a peak current 16.11 μA, and RS gave a peak at +0.092 V with peak current 4.48 μA. For a ternary mixture, three sharp and well-defined peaks were found at −0.005, +0.1, and +0.49 V with peak currents 9.07, 12.36, and 5.56 μA, respectively. At GLY-HBPE, in CV, HQ gave anodic and cathodic peaks at +0.026 and −0.034 V, respectively. CC gave anodic and cathodic peaks at +0.112 and +0.048 V, respectively. RS gave only an anodic peak at +0.484 V. For the ternary mixture, HQ, CC, and RS gave three sharp and well-defined anodic peaks at +0.084, +0.182, and +0.568 V with peak currents of 23.51, 20.42, and 17.91 μA, respectively. Two cathodic peaks were found at +0.01 and +0.13 V with peak currents of 15.11 and



https://doi.org/10.1021/acsomega.2c03651
ACS Omega 2022, 7, 29391−29405

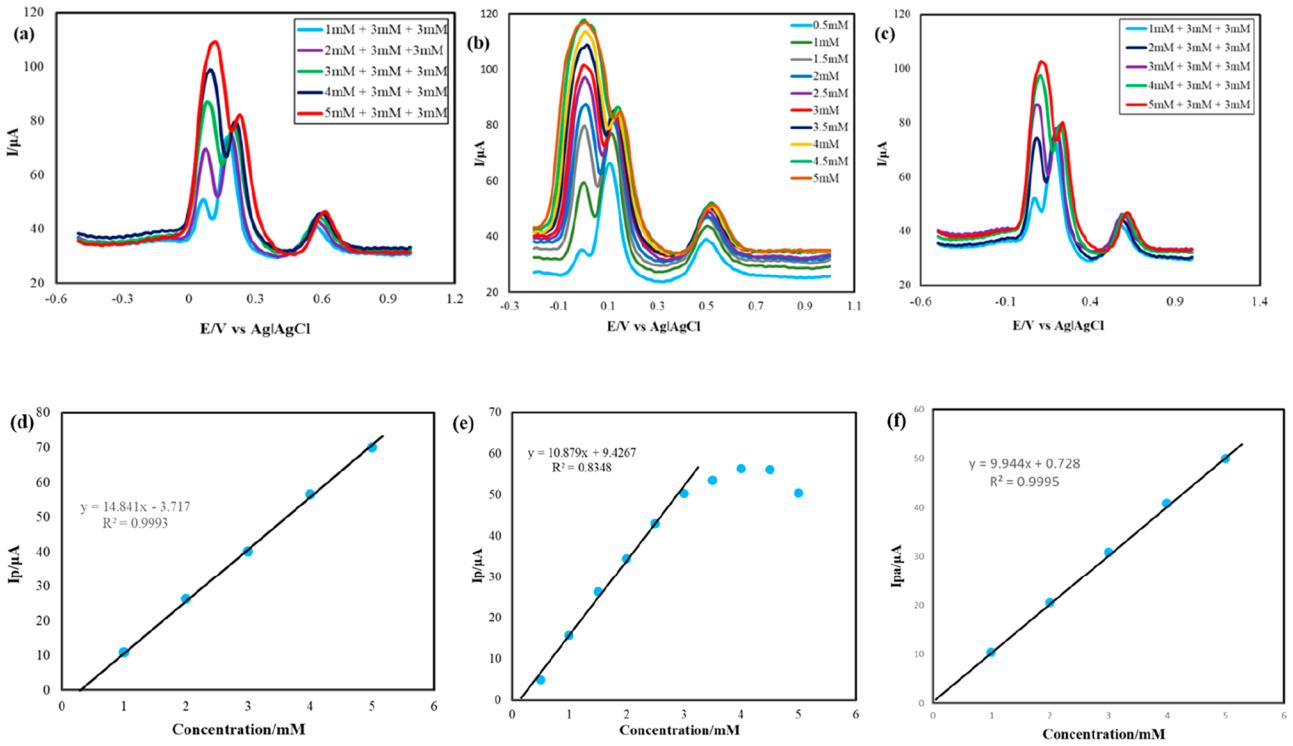


**Figure 7.** DPV for quantitative estimation of HQ in the presence of CC and RS at 50 $mVs^{-1}$ on (a) bare HBPE, (b) GLY-HB, and (c) ASA-HB. Calibration curve for estimation of HQ in the presence of CC and RS (current response with variation of concentration) at (d) bare HBPE, (e) GLY-HB, and (f) ASA-HB.

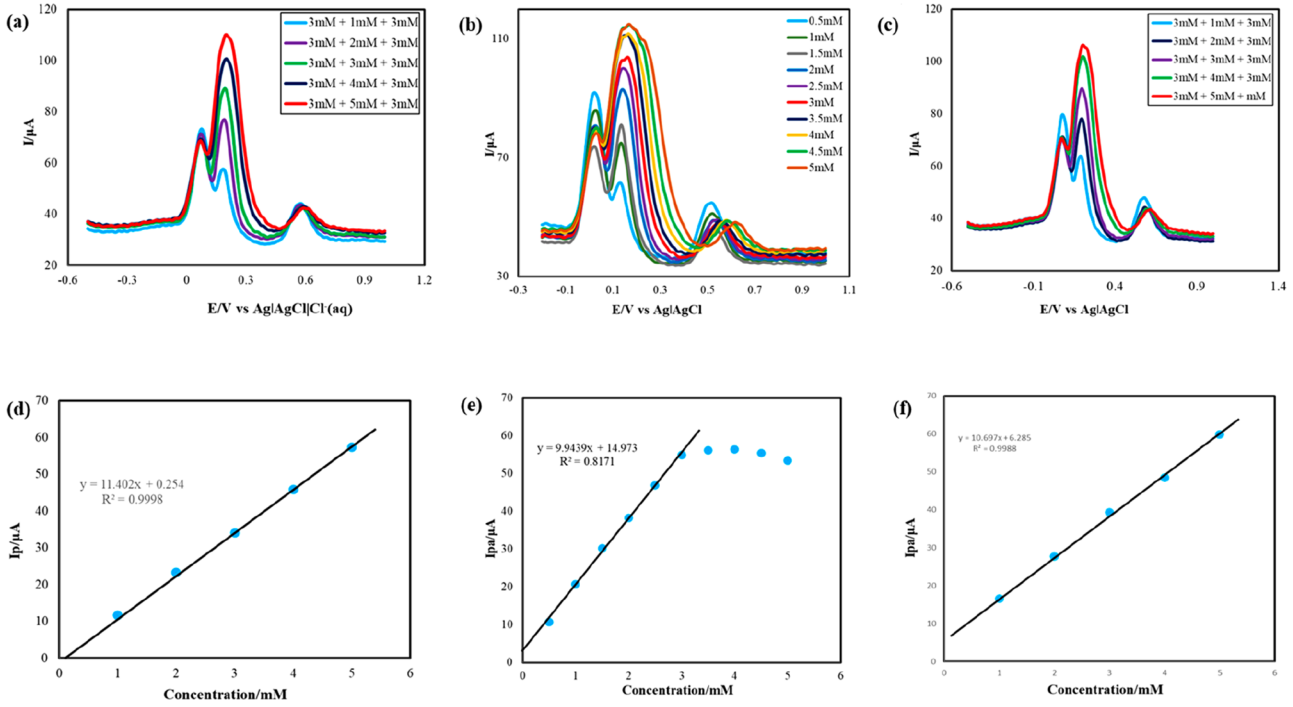


**Figure 8.** DPV for quantitative estimation of CC in the presence of HQ and RS at 50 $mVs^{-1}$ on (a) bare HBPE, (b) GLY-HB, and (c) ASA-HB. Calibration curve for estimation of CC in the presence of HQ and RS (current response with variation of concentration) at (d) bare HBPE, (e) GLY-HB, and (f) ASA-HB.

11.68 $\mu$A, respectively. In DPV, for a single mixture, HQ gave a peak at +0.00 V, CC gave a peak at +0.085 V, and RS gave a peak at +0.455 V. For the ternary mixture, three sharp and well-defined peaks were observed at +0.00, +0.105, and +0.485 V with peak currents of 19.08, 23.29, and 8.15 $\mu$A, respectively. At ASA-HBPE, in CV, HQ gave anodic and cathodic peaks at +0.03 and −0.028 V, respectively. CC gave anodic and cathodic peaks at +0.132 and +0.06 V, respectively. RS gave only an anodic peak at +0.514 V. For th eternary mixture, HQ, CC, and RS gave three sharp and well-defined anodic peaks at



https://doi.org/10.1021/acsomega.2c03651
ACS Omega 2022, 7, 29391−29405

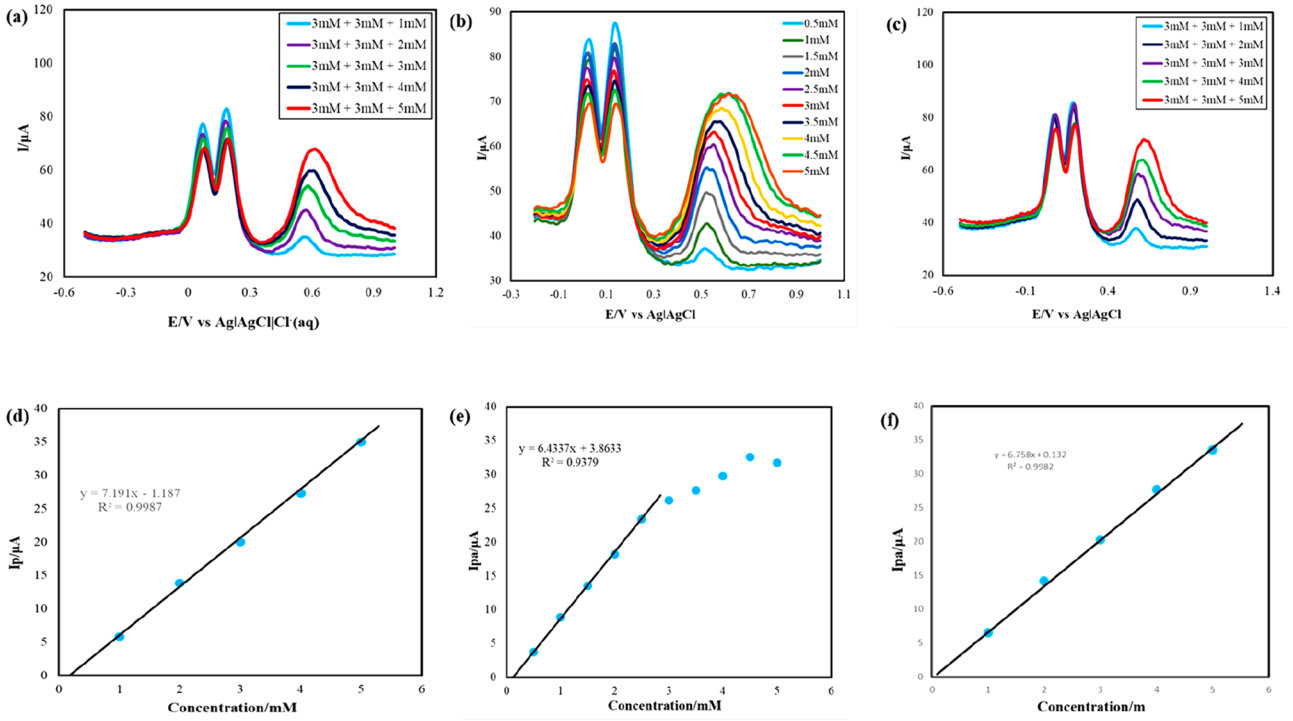


**Figure 9.** DPV for quantitative estimation of RS in the presence of HQ and CC at 50 $mVs^{-1}$ on (a) bare HBPE, (b) GLY-HB, and (c) ASA-HB. Calibration curve for estimation of RS in the presence of HQ and CC (current response with variation of concentration) at (d) bare HBPE, (e) GLY-HB, and (f) ASA-HB.

+0.082, +0.188, and +0.57 V, respectively. Two cathodic peaks were found at +0.01 and +0.132, respectively. In DPV, for a single mixture, HQ gave a peak at +0.01 V, CC gave a peak at +0.105 V, and RS gave a peak at +0.485 V, and in the ternary mixture, three sharp and well-defined peak at −0.295, −0.19, and +0.195 V were observed, respectively; this indicates good separating ability for quantitative detection.

**Quantitative Detection of HQ in the Presence of CC and RS.** DPV was performed on the ternary mixture of HQ, CC, and RS (1:1:1) in PBS (pH 6.8) at HBPE (Figure 7a). The ternary solution was prepared where CC and RS were kept constant at concentration 3 mM, and the concentration of HQ was increased by adding a successive amount of HQ in the ternary solution. Concentration versus current curve (Figure 7d) was drawn for different concentrations of HQ in the presence of constant amounts of CC and RS. The curve maintains the linearity with concentration of HQ. This curve can be used to determine HQ in the presence of CC and RS quantitatively in a ternary mixture. This concentration versus current curve can be used for quantitative estimation of HQ simultaneously from the ternary mixture. In the case of HQ the peak current increases approximately 14.783 $\mu$A/mM. The LOD (S/N = 3), LOQ (S/N = 10), and sensitivity were found to be 12.473 $\mu$M (±1.6 $\mu$M), 41.58 $\mu$M (±5.21 $\mu$M), and 470.481 $\mu$A/mM/$cm^2$, respectively. A similar experiment was performed at GLY-HBPE, DPVs are shown in Figure 7b, and the current was increased by adding successive amounts of HQ in the presence of constant CC and RS. The concentration versus current curve (Figure 7e)) was drawn for different concentrations of HQ in the presence of constant amounts of CC and RS in the ternary mixture. The curve maintains the linearity with the concentration of HQ, and the peak current increases approximately 11.462 $\mu$A/mM. The LOD (S/N = 3), LOQ (S/N = 10), and sensitivity were found to be 5.498 $\mu$M (±2.19 $\mu$M), 18.32 $\mu$M (±7.31 $\mu$M), and 364.785 $\mu$A/mM/$cm^2$, respectively. At ASA-HBPE, the current was also increased for successive amounts of HQ in the presence of CC and RS as confirmed by DPVs (Figure 7 c), and the peak current increased approximately 11.766 $\mu$A/mM. The concentration versus current curve is shown in Figure 7f. The LOD (S/N = 3), LOQ (S/N = 10), and sensitivity were found to be 22.459 $\mu$M (±3.34 $\mu$M), 74.86 $\mu$M (±11.13 $\mu$M), and 374.483 $\mu$A/mM/$cm^2$, respectively, after simultaneous detection from a ternary mixture.

**Quantitative Detection of CC in the Presence of HQ and RS.** Experiments similar to the previous one were carried out for the estimation of CC in the presence HQ and RS. DPVs were carried out at HBPE (Figure 8a), GLY-HB (Figure 8b), and ASA-HB (Figure 8c). For all three electrodes, the current was increased linearly with successive amounts of CC in the presence of HQ and RS. The concentration versus current curve was drawn for HBPE (Figure 8d), GLY-HB (Figure 8e), and ASA-HB (Figure 8f). At HBPE, GLY-HB, and ASA-HB, the peak current of CC was increased approximately 11.43, 8.851, and 10.372 $\mu$A/mM, respectively, the LOD (S/N = 3) was 16.132 $\mu$M (±2.02 $\mu$M), 7.119 $\mu$M (±2.16 $\mu$M), and 25.478 $\mu$M (±3.79 $\mu$M), respectively, LOQ (S/N = 10) was 53.77 $\mu$M (±6.74 $\mu$M), 23.72 $\mu$M (±7.18 $\mu$M), and 84.93 $\mu$M (±12.63 $\mu$M), respectively, and the sensitivity was 363.781, 281.712, and 330.108 $\mu$A/mM/$cm^2$, respectively, in the presence of 3 mM HQ and RS.

**Quantitative Detection of RS in the Presence of HQ and CC.** DPVs were also performed for quantitative detection of RS in the presence of 3 mM HQ and CC at HBPE (Figure 9a), GLY-HB (Figure 9b), and ASA-HB (Figure 9c). For all cases, the current was linearly increased for successive amounts of RS in the presence of HQ and CC, and the concentration


https://doi.org/10.1021/acsomega.2c03651
ACS Omega 2022, 7, 29391−29405

versus current curve was drawn for HBPE (Figure 9d), GLY-HB (Figure 9e, and ASA-HB (Figure 9f).

At HBPE, GLY-HB, and ASA-HB, the peak current of RS was increased approximately 7.303, 4.259, and 6.899 $\mu$A/mM, respectively, the LOD (S/N = 3) was 25.25 $\mu$M (±3.1 $\mu$M), 14.794 $\mu$M (±5.9 $\mu$M), and 38.303 $\mu$M (±5.69 $\mu$M), respectively, LOQ (S/N = 10) was 84.17 $\mu$M (±10.56 $\mu$M), 49.31 $\mu$M (±19.68 $\mu$M), and 127.68 $\mu$M (±18.98 $\mu$M), respectively, and the sensitivity was 232.416, 135.560, and 219.573 $\mu$A/mM/cm$^2$, respectively, in the presence of 3 mM HQ and RS.

A list containing the sensitivity and LOD and LOQ of bare HBPE, GLY-HB, and ASA-HB is placed in Table 1. It is seen that bare HBPE has the highest sensitivity and GLY-HB has the lowest detection limit in all cases.

**Table 1. Sensitivity and LOD Comparison among Bare HBPE, GLY-HB, and ASA-HB**

| electrode | DHBIs | sensitivity ($\mu$A/mM/cm$^2$) | LOD ($\mu$M) | LOQ ($\mu$M) |
|---|---|---|---|---|
| bare HBPE | HQ | 470.481 | 12.473 ± 1.6 | 41.58 ± 5.21 |
| | CC | 363.781 | 16.132 ± 2.02 | 53.77 ± 6.74 |
| | RS | 232.416 | 25.245 ± 3.1 | 84.17 ± 10.56 |
| GLY-HB | HQ | 364.785 | 5.498 ± 2.19 | 18.32 ± 7.31 |
| | CC | 281.712 | 7.119 ± 2.16 | 23.72 ± 7.18 |
| | RS | 135.560 | 14.794 ± 5.9 | 49.31 ± 19.68 |
| ASA-HB | HQ | 374.483 | 22.459 ± 3.34 | 74.86 ± 11.13 |
| | CC | 330.108 | 25.478 ± 3.79 | 84.93 ± 12.63 |
| | RS | 219.574 | 38.303 ± 5.69 | 127.68 ± 18.98 |

**Electrochemical Impedance Study.** A 1 mM ternary solution of DHBIs was taken as a probe to depict the electrochemical alteration of HBPE after modification with GLY and ASA. After investigating the CVs, the value of the potential was taken at 1.0 V for permitting the redox behavior. The solution resistances ($R_s$) for all electrodes are nearly similar; and the values of $R_s$ were 127.07, 115.42, and 87.79 Ω for HBPE, GLY-HB, and ASA-HB, respectively (Figure 10). The charge-transfer resistance ($R_{ct}$) of the DHBIs redox couple at all of the electrodes was very high, supporting the surface properties obtained from the SEM and EDX analysis. Besides, $R_{ct}$ of DHBIs at HBPE was comparatively smaller than those of GLY-HB and ASA-HB, which explains the reason for obtaining almost similar results in quantitative detections.

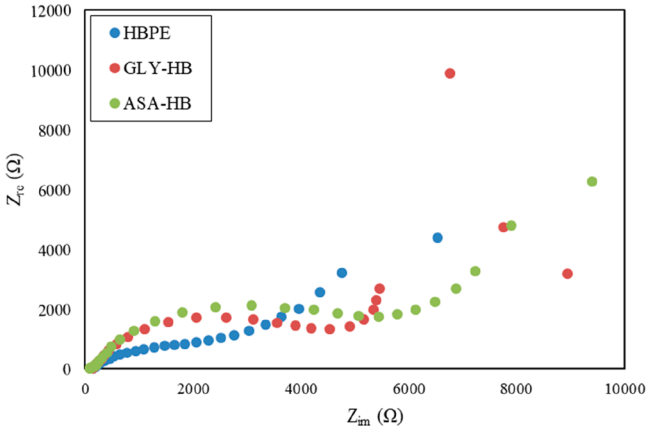


**Figure 10.** EIS plots of 1 mM HQ, CC, and RS in PBS at HBPE, GLY-HB, and ASA-HB.

**Fukui Function Analysis.** From Figure 2, it is seen that the background current of HBPE is higher than that of ASA-HB and lower than that of GLY-HB. This probability could be checked by Fukui function theory. The Fukui function theory gives us informationthat atoms in a molecule have a large tendency to either lose or accept an electron, which in turn indicates that there are a lot of possibilities to endure a nucleophilic and electrophilic attack. The theoretical calculations were done by the DFT/wB97XD/6-311+g(d,p) level of theory using Gaussian 16 software package. The Fukui function is defined as

$$F = ((\delta\rho(r))/\delta N)r \quad (1)$$

where, $\rho(r)$ is the electron density, $N$ is the number of electrons, and $r$ is the external potential. The Fukui function is a local reactivity descriptor which gives the preferred region of a species where other molecule will go and get oxidized or reduced when the number of electron is modified. The corresponding Fukui functions on the $j$th atom site are given as

$$f_j^+ = Q_j(N+1) - Q_j(N) \quad (2)$$

$$f_j^- = Q_k(N) - Q_j(N-1) \quad (3)$$

$$f_j^0 = \frac{1}{2}[Q_j(N+1) - Q_j(N-1)] \quad (4)$$

$$\Delta f(r) = [f_j^+ - f_j^-] \quad (5)$$

Here, $f_j^-$, $f_j^+$, and $f_j^0$ represent the electrophilic, nucleophilic, and free radical on the reference molecule, respectively. $Q_j$ is the atomic charge at the $j$th atomic site for the neutral (N), anionic (N+1), or (N−1) chemical species. The dual descriptor $\Delta f(r)$ is the difference between the nucleophilic and electrophilic Fukui function. The site is favored by nucleophilic attack when $\Delta f(r) > 0$ and electrophilic attack when $\Delta f(r) < 0$.[59−62]

Figures 11−13 represents the atomic arrangements of the graphite sheet of the bare HBPE surface, glycine, and aspartic acid, respectively, and Tables 2−4 represents the values of Fukui functions for the atoms of the graphite sheet, glycine, and aspartic acid, respectively. Mulliken population analysis indicated the local reactivity of a molecule. As a dual descriptor, the graphite molecule has nucleophilic sites [$\Delta f(r) > 0$] C1, C4, C6, C8, C10, C11, C15 and electrophilic sites [$\Delta f(r) < 0$] C2, C3, C5, C7, C9, C12, C13, C14, C16. The glycine molecule has nucleophilic sites H2, C3, O4, O5, N7, H8, H9, H10 and electrophilic sites C1, H6. The aspartic

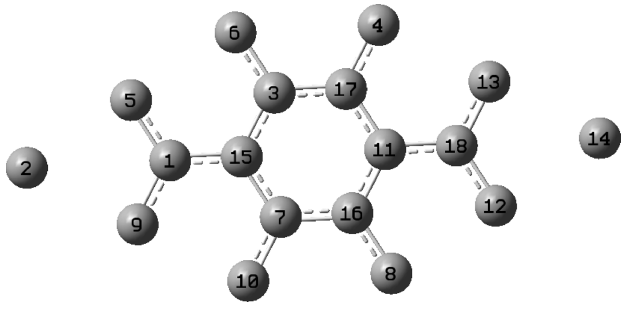


**Figure 11.** Structure of graphite sheet (bare HBPE surface).



https://doi.org/10.1021/acsomega.2c03651
ACS Omega 2022, 7, 29391−29405

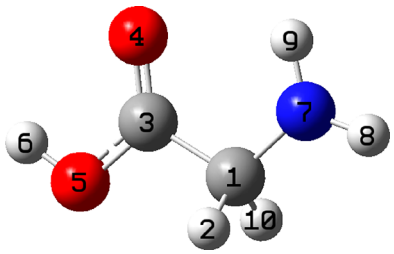


**Figure 12.** Structure of glycine.

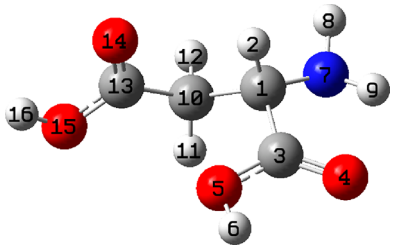


**Figure 13.** Structure of aspartic acid.

acid molecule has nucleophilic sites H2, O5, N7, H8, H9, H11, H12, C13, O14, O15, H16 and electrophilic sites C1, C3, O4, H6, C10. As a bare surface, the graphite sheet has both nucleophilic and electrophilic sites with foreign particles and new fresh surface after each rubbing while glycine and aspartic acid molecule has fixed nucleophilic and electrophilic sites very close to each other. When the HBPE bare surface is modified by GLY or ASA, the atoms of GLY and ASA affects the nucleophilic and/or electrophilic tendencies of the molecules of graphite sheet. It could be possible that, after modification, some active sites of GLY-HB were blocked, responsible for more background current while for ASA-HB, more active site are generates for easy electron transfer.[52−54]

**Cost-Benefit Analysis.** Conventional commercial electrodes, like GCE (165−235 USD), platinum electrode (212−283 USD), and gold electrode (200−260 USD), etc., are very costly and unavailable in the local market in Bangladesh. In order to get those, import from foreign markets is necessary and requires a minimum 3−6 months for delivery. But HBPE, GLY-HBm and ASA-HB are unbelievably cheap and very available. The cost of one HBPE is about 0.059 USD, one GLY-HB or ASA-HB electrode is about 0.083 USD. In the same laboratory one previous researcher fabricated modified 2B PGE by IL, namely BIHP, in order to detect HQ, CC, and RS simultaneously from aqueous solution. Moreover, she got some exciting results, but IL is very costly and unavailable, unlike AAs.[2]

**Interference Studies.** During the detection of HQ, CC, and RS, various species in the environment may be present and interfere with the readings. Phenol and other phenolic isomers are the top interfering substances Thus, the peak currents of HQ, CC, and RS were further examined in the presence of phenol, 2-nitrophenol, and 4-nitrophenol as well as in the presence of some cations and anions such as $Ca^{2+}$, $Mg^{2+}$, $NH_4^+$, $Zn^{2+}$, $K^+$, $Na^+$, $Mn^{2+}$, $Cu^{2+}$, $Pb^{2+}$, $Fe^{2+}$, $SO_4^{2-}$, $Cl^-$, and $NO_3^-$ at the proposed HBPE, GLY-HB, and ASA-HB electrodes. First, the same concentrations of these interfering species were taken with DHBIs, and the current responses were monitored. It was seen that those species did not interfere with the oxidation peaks of DHBIs. The current responses were further monitored, having 10 times greater the concentration of interfering species than the concentration of DHBIs, and it was seen that even at such a high concentration they did not interfere with the oxidation peaks of DHBIs. The interference test is shown in Table 5, signifying the dependability of HBPE, GLY-HB, and ASA-HB for the detection of DHBIs in aqueous systems.

*Real Sample Analysis.* Several researchers have reported that HQ, CC, and RS may coexist in real samples, which need to be quantified.[1−5] They used local tap water,[5,63] river water,[64] and tea samples[65] for the recovery test instead of using real samples. In this study, we mixed HQ, CC, and RS in tap water as different ratios as an alternative to the real samples to check the usability of HBPE, GLY-HB, and ASA-HB. The peak currents per mM found using distilled water were compared with peak currents per mM found using local tap water. Table 6 represents the recovery test. All the three electrodes showed good recovery.

*Feasibility of Use.* It is anticipated that a sensor be fit for frequent use in a highly reproducible way. One of the

**Table 2. Fukui Functions for the Atoms of Graphite Sheet Using Mulliken Population Analysis**

| | Mulliken atomic charges | | | Fukui functions | | | |
|---|---|---|---|---|---|---|---|
| atoms | $q(N+1)$ | $q(N)$ | $q(N-1)$ | $f_j^+$ | $f_j^-$ | $f_j^0$ | $\Delta f(r)$ |
| C1 | 0.008 | −0.043 | −0.066 | 0.051 | 0.023 | 0.037 | 0.028 |
| C2 | 0.005 | 0.169 | 0.305 | −0.164 | −0.136 | −0.15 | −0.028 |
| C3 | 0.349 | 0.416 | 0.454 | −0.067 | −0.038 | −0.0525 | −0.029 |
| C4 | −0.486 | −0.462 | −0.394 | −0.024 | −0.068 | −0.046 | 0.044 |
| C5 | −0.231 | −0.108 | −0.04 | −0.123 | −0.068 | −0.0955 | −0.055 |
| C6 | −0.486 | −0.462 | −0.394 | −0.024 | −0.068 | −0.046 | 0.044 |
| C7 | 0.349 | 0.416 | 0.454 | −0.067 | −0.038 | −0.0525 | −0.029 |
| C8 | −0.486 | −0.462 | −0.394 | −0.024 | −0.068 | −0.046 | 0.044 |
| C9 | −0.231 | −0.108 | −0.04 | −0.123 | −0.068 | −0.0955 | −0.055 |
| C10 | −0.486 | −0.462 | −0.394 | −0.024 | −0.068 | −0.046 | 0.044 |
| C11 | 0.223 | 0.183 | 0.221 | 0.04 | −0.038 | 0.001 | 0.078 |
| C12 | −0.231 | −0.108 | −0.04 | −0.123 | −0.068 | −0.0955 | −0.055 |
| C13 | −0.231 | −0.108 | −0.04 | −0.123 | −0.068 | −0.0955 | −0.055 |
| C14 | 0.005 | 0.169 | 0.305 | −0.164 | −0.136 | −0.15 | −0.028 |
| C15 | 0.223 | 0.183 | 0.221 | 0.04 | −0.038 | 0.001 | 0.078 |
| C16 | 0.349 | 0.416 | 0.454 | −0.067 | −0.038 | −0.0525 | −0.029 |



https://doi.org/10.1021/acsomega.2c03651
ACS Omega 2022, 7, 29391−29405

Table 3. Fukui Functions for the Atoms of Glycine Using Mulliken Population Analysis

| | Mulliken atomic charges | | | Fukui functions | | | |
|---|---|---|---|---|---|---|---|
| atoms | $q(N+1)$ | $q(N)$ | $q(N-1)$ | $f_j^+$ | $f_j^-$ | $f_j^0$ | $\Delta f(r)$ |
| C1 | −2.676 | −0.238 | −0.42 | −2.438 | 0.182 | −1.128 | −2.62 |
| H2 | 0.192 | 0.178 | 0.305 | 0.014 | −0.127 | −0.0565 | 0.141 |
| C3 | 0.616 | 0.174 | 0.231 | 0.442 | −0.057 | 0.1925 | 0.499 |
| O4 | −0.106 | −0.321 | −0.252 | 0.215 | −0.069 | 0.073 | 0.284 |
| O5 | 0.542 | −0.217 | −0.158 | 0.759 | −0.059 | 0.35 | 0.818 |
| H6 | 0.174 | 0.282 | 0.334 | −0.108 | −0.052 | −0.08 | −0.056 |
| N7 | −0.451 | −0.601 | −0.105 | 0.15 | −0.496 | −0.173 | 0.646 |
| H8 | 0.222 | 0.278 | 0.395 | −0.056 | −0.117 | −0.0865 | 0.061 |
| H9 | 0.293 | 0.286 | 0.366 | 0.007 | −0.08 | −0.0365 | 0.087 |
| H10 | 0.192 | 0.178 | 0.305 | 0.014 | −0.127 | −0.0565 | 0.141 |

Table 4. Fukui Functions for the Atoms of Aspartic Acid Using Mulliken Population Analysis

| | Mulliken atomic charges | | | Fukui functions | | | |
|---|---|---|---|---|---|---|---|
| atoms | $q(N+1)$ | $q(N)$ | $q(N-1)$ | $f_j^+$ | $f_j^-$ | $f_j^0$ | $\Delta f(r)$ |
| C1 | −0.509 | −0.216 | −0.365 | −0.293 | 0.149 | −0.072 | −0.442 |
| H2 | 0.193 | 0.246 | 0.341 | −0.053 | −0.095 | −0.074 | 0.042 |
| C3 | −0.963 | 0.133 | 0.196 | −1.096 | −0.063 | −0.5795 | −1.033 |
| O4 | −0.438 | −0.332 | −0.234 | −0.106 | −0.098 | −0.102 | −0.008 |
| O5 | −0.151 | −0.187 | −0.148 | 0.036 | −0.039 | −0.0015 | 0.075 |
| H6 | 0.239 | 0.312 | 0.347 | −0.073 | −0.035 | −0.054 | −0.038 |
| N7 | 0.177 | −0.452 | −0.046 | 0.629 | −0.406 | 0.1115 | 1.035 |
| H8 | 0.168 | 0.246 | 0.343 | −0.078 | −0.097 | −0.0875 | 0.019 |
| H9 | 0.238 | 0.264 | 0.332 | −0.026 | −0.068 | −0.047 | 0.042 |
| C10 | −0.587 | −0.261 | −0.319 | −0.326 | 0.058 | −0.134 | −0.384 |
| H11 | 0.188 | 0.231 | 0.289 | −0.043 | −0.058 | −0.0505 | 0.015 |
| H12 | 0.217 | 0.215 | 0.253 | 0.002 | −0.038 | −0.018 | 0.04 |
| C13 | 0.419 | −0.013 | 0.02 | 0.432 | −0.033 | 0.1995 | 0.465 |
| O14 | −0.298 | −0.312 | −0.204 | 0.014 | −0.108 | −0.047 | 0.122 |
| O15 | −0.153 | −0.156 | −0.116 | 0.003 | −0.04 | −0.0185 | 0.043 |
| H16 | 0.259 | 0.279 | 0.311 | −0.02 | −0.032 | −0.026 | 0.012 |

electrodes of HBPE, GLY-HB, and ASA-HB used in the tests described above was stored in an empty beaker for 10 weeks without any drop in performance during use.

## MATERIALS AND METHODS

**Instrumentation and Chemicals.** The electrochemical studies (CV and DPV) were performed with a potentiostat ($\mu$-stat 8000, DropSens, Spain). Graphite pencil, grade HB (local market), was used as working electrode. Ag|AgCl|$Cl^-$(aq) was used as the reference electrode. A coil of Pt wire was the counter electrode. A magnetic stirrer (Glassgo, India) with a Teflon-coated magnetic bar was used. A pH meter (EZODO, Taiwan) was employed for maintaining the pH of the solutions. Solutions were prepared using ordinary laboratory glassware. An electronic balance (Model: HR-200, Japan) was used to weigh the required amount of compounds. The surface morphology was investigated with the help of SEM (JEOL, USA) measurements equipped with a JEOL EDX spectrometer. The samples for EDX were molded as disks and placed on a carbon tape. Some accessories like an anticutter, offset paper, polishing pads, etc. were also used.

All chemicals and solvents used in the analysis were of analytical grade: catechol (BDH, UK), hydroquinone (BDH, UK), resorcinol (BDH, UK), sodium dihydrogen phosphate, $NaH_2PO_4$ (Sigma-Aldrich, USA), disodium hydrogen phosphate, $Na_2HPO_4$ (Sigma-Aldrich, USA), L-amino acids reference standard kit (SRL India), graphite pencil of grade HB (Local market, Bangladesh). 99.997% dry nitrogen (BOC, Bangladesh) was used for purging purposes. For cleaning and all other purposes distilled water was used.

**Preparation of HBPE, Gly-HB, and ASA-HB Electrodes.** The working electrode used in this study was HBPE. It was made by cutting the wooden part of the two side of the pencil with a sharp anticutter. Then it was washed with distilled water and dried by air. Then one part is painted using an insulating dye, and the end of the spherical surface was left free and then polished by rubbing it on a smooth paper. At this point, the electrode surface looked like a shiny black mirror. Another part was used to make the connection with the potentiostat.

A 0.0375 g (0.01 M) sample of glycine (Gly) was weighed and kept in 50 mL of PBS (0.2 M, pH = 6.8) in a beaker. The beakers were covered with parafilm, placed in an ultrasonic bath for 1 h, and then placed on a magnetic stirrer machine and stirred for 3 h at 60 °C. Prior to electrochemical modification, the bare HBPE with a diameter of 2 mm was polished on a paper. Then it was rinsed with water. The electrode was treated with cyclic scanning between −1.0 V and +1.7 V at a scan rate of 300 mV $s^{-1}$ by 15 scans. After modification, the modified electrode was electroactivated by cyclic voltammetry from −0.5 to +1.0 V at 100 $mVs^{-1}$ in pH 6.8 phosphate buffer solution. Then the electrode was used followed by washing with distilled water and referred to as GLY-HB. Similar processes were done for the preparation of ASA-HB. A 0.0665 g (0.01 M) portion of aspartic acid (ASA)



https://doi.org/10.1021/acsomega.2c03651
ACS Omega 2022, 7, 29391−29405

**Table 5. Possible Interference Test**

| interfering substance | current ratios (HQ) | current ratios (CC) | current ratios (RS) |
|---|---|---|---|
| phenol | 0.92[a](H) | 0.97[a](H) | 0.97[a](H) |
| | 0.96[b](H) | 0.96[b](H) | 0.95[b](H) |
| | 0.91[a](G) | 0.98[a](G) | 0.96[a](G) |
| | 0.95[b](G) | 0.96[b](G) | 0.95[b](G) |
| | 0.91[a](A) | 0.98[a](A) | 0.98[a](A) |
| | 0.92[b](A) | 0.98[b](A) | 0.97[b](A) |
| 2-nitrophenol | 0.96[a] (H) | 0.98[a](H) | 0.98[a](H) |
| | 0.96[b](H) | 0.97[b](H) | 0.91[b](H) |
| | 0.92[a](G) | 0.96[a](G) | 0.96[a](G) |
| | 0.97[b](G) | 0.98[b](G) | 0.95[b](G) |
| | 0.93[a](A) | 0.98[a](A) | 1.01[a](A) |
| | 0.93[b](A) | 1.03[b](A) | 0.98[b](A) |
| 4-nitrophenol | 1.05[a] (H) | 0.98[a](H) | 0.96[a](H) |
| | 1.03[b](H) | 0.98[b](H) | 0.92[b](H) |
| | 0.91[a](G) | 1.00[a](G) | 0.96[a](G) |
| | 0.95[b](G) | 1.02[b](G) | 1.03[b](G) |
| | 0.96[a](A) | 0.98[a](A) | 1.01[a](A) |
| | 0.93[b](A) | 1.03[b](A) | 0.94[b](A) |
| $Ca^{2+}$ | 0.94[a] (H) | 0.96[a](H) | 0.99[a](H) |
| | 1.02[b](H) | 0.98[b](H) | 1.01[b](H) |
| | 0.99[a](G) | 1.02[a](G) | 0.99[a](G) |
| | 1.02[b](G) | 0.99[b](G) | 1.03[b](G) |
| | 0.99[a](A) | 0.92[a](A) | 0.94[a](A) |
| | 0.98[b](A) | 0.98[b](A) | 1.00[b](A) |
| $Mg^{2+}$ | 1.00[a] (H) | 0.98[a](H) | 1.00[a](H) |
| | 1.02[b](H) | 0.98[b](H) | 1.07[b](H) |
| | 0.99[a](G) | 1.04[a](G) | 1.02[a](G) |
| | 0.98[b](G) | 0.96[b](G) | 1.01[b](G) |
| | 1.00[a](A) | 0.96[a](A) | 0.96[a](A) |
| | 0.99[b](A) | 1.00[b](A) | 0.91[b](A) |
| $NH_4^+$ | 0.98[a] (H) | 0.92[a](H) | 0.99[a](H) |
| | 0.99[b](H) | 0.94[b](H) | 1.01[b](H) |
| | 1.02[a](G) | 0.98[a](G) | 0.95[a](G) |
| | 0.95[b](G) | 0.98[b](G) | 1.07[b](G) |
| | 0.99[a](A) | 0.95[a](A) | 0.98[a](A) |
| | 1.03[b](A) | 1.00[b](A) | 0.95[b](A) |
| $Zn^{2+}$ | 0.99[a] (H) | 0.98[a](H) | 1.02[a](H) |
| | 1.08[b](H) | 0.97[b](H) | 0.98[b](H) |
| | 0.95[a](G) | 0.98[a](G) | 1.01[a](G) |
| | 0.96[b](G) | 1.00[b](G) | 1.02[b](G) |
| | 1.05[a](A) | 0.96[a](A) | 0.98[a](A) |
| | 0.96[b](A) | 1.02[b](A) | 0.95[b](A) |
| $K^+$ | 0.92[a] (H) | 0.96[a](H) | 0.95[a](H) |
| | 0.92[b](H) | 1.02[b](H) | 1.03[b](H) |
| | 0.99[a](G) | 1.01[a](G) | 1.07[a](G) |
| | 1.02[b](G) | 1.05[b](G) | 1.05[b](G) |
| | 1.02[a](A) | 0.98[a](A) | 0.96[a](A) |
| | 1.00[b](A) | 1.00[b](A) | 0.98[b](A) |
| $Na^+$ | 0.98[a] (H) | 0.98[a](H) | 1.00[a](H) |
| | 1.02[b](H) | 0.98[b](H) | 1.04[b](H) |
| | 0.96[a](G) | 1.01[a](G) | 1.02[a](G) |
| | 0.97[b](G) | 0.96[b](G) | 1.03[b](G) |
| | 1.02[a](A) | 1.03[a](A) | 1.03[a](A) |
| | 0.99[b](A) | 1.03[b](A) | 0.97[b](A) |
| $Mn^{2+}$ | 0.94[a] (H) | 0.98[a](H) | 0.97[a](H) |
| | 1.03[b](H) | 0.98[b](H) | 1.02[b](H) |
| | 1.00[a](G) | 1.04[a](G) | 1.05[a](G) |
| | 0.97[b](G) | 0.97[b](G) | 1.06[b](G) |
| | 1.03[a](A) | 0.98[a](A) | 0.98[a](A) |
| | 1.02[b](A) | 1.03[b](A) | 0.95[b](A) |
| $Cu^{2+}$ | 0.98[a] (H) | 0.98[a](H) | 1.02[a](H) |
| | 1.05[b](H) | 0.98[b](H) | 1.06[b](H) |
| | 0.96[a](G) | 1.02[a](G) | 1.03[a](G) |
| | 0.98[b](G) | 0.96[b](G) | 0.98[b](G) |
| | 1.00[a](A) | 0.98[a](A) | 0.94[a](A) |
| | 1.02[b](A) | 1.00[b](A) | 0.97[b](A) |
| $Pb^{2+}$ | 0.95[a] (H) | 0.98[a](H) | 0.99[a](H) |
| | 0.99[b](H) | 0.98[b](H) | 1.01[b](H) |
| | 0.99[a](G) | 0.98[a](G) | 0.97[a](G) |
| | 0.99[b](G) | 0.96[b](G) | 1.03[b](G) |
| | 1.03[a](A) | 0.96[a](A) | 0.96[a](A) |
| | 1.05[b](A) | 0.99[b](A) | 0.93[b](A) |
| $Fe^{2+}$ | 0.95[a] (H) | 0.96[a](H) | 0.98[a](H) |
| | 1.02[b](H) | 0.98[b](H) | 1.01[b](H) |
| | 0.99[a](G) | 1.03[a](G) | 0.99[a](G) |
| | 0.98[b](G) | 0.99[b](G) | 0.97[b](G) |
| | 1.03[a](A) | 0.97[a](A) | 0.96[a](A) |
| | 0.98[b](A) | 1.00[b](A) | 0.96[b](A) |
| $SO_4^{2-}$ | 0.95[a](H) | 0.96[a](H) | 0.98[a](H) |
| | 0.95[b](H) | 0.98[b](H) | 0.97[b](H) |
| | 0.98[a](G) | 1.04[a](G) | 1.01[a](G) |
| | 0.98[b](G) | 1.01[b](G) | 1.03[b](G) |
| | 0.98[a](A) | 1.00[a](A) | 0.96[a](A) |
| | 1.04[b](A) | 1.00[b](A) | 0.99[b](A) |
| $Cl^-$ | 0.97[a] (H) | 0.95[a](H) | 0.99[a](H) |
| | 1.00[b](H) | 0.98[b](H) | 0.97[b](H) |
| | 0.99[a](G) | 0.94[a](G) | 1.04[a](G) |
| | 0.98[b](G) | 0.98[b](G) | 1.03[b](G) |
| | 1.02[a](A) | 1.00[a](A) | 1.02[a](A) |
| | 0.99[b](A) | 1.00[b](A) | 0.99[b](A) |
| $NO^{3-}$ | 1.01[a] (H) | 1.06[a](H) | 1.00[a](H) |
| | 1..4[b](H) | 0.98[b](H) | 1.01[b](H) |
| | 1.02[a](G) | 1.01[a](G) | 0.99[a](G) |
| | 0.95[b](G) | 0.96[b](G) | 1.03[b](G) |
| | 1.00[a](A) | 0.96[a](A) | 0.99[a](A) |
| | 1.00[b](A) | 1.01[b](A) | 0.94[b](A) |

[a]Ratio of currents of 1 mM DHBIs compared with 1 mM DHBIs with same concentration of interfering substances [b]Ratio of currents of 1 mM DHBIs compared with 1 mM DHBIs with ten times more the concentration of interfering substances (H), (G), and (A) represent the results for HBPE, GLY-HB, and ASA-HB respectively.

was weighed and kept in 50 mL of PBS (0.2 M, pH = 6.8) in another beaker, and the modification process was followed by the modification of GLY-HB electrode.

## CONCLUSION

A trailblazing method was projected for the simultaneous determination of DHBIs in an aqueous system. PGE, grade HB, was used for the fabrication of a simple, cost-effective, sensitive, and selective electrochemical sensing platform and named HBPE. Surface morphology was analyzed by SEM and EDX. The surface of bare HBPE was electrochemically modified by AAs (GLY or ASA). CV and DPV were employed for the simultaneous detection of DHBIs in single, binary, and ternary mixtures. All electrodes, bare HBPE, as well as GLY-



https://doi.org/10.1021/acsomega.2c03651
ACS Omega 2022, 7, 29391−29405

**Table 6. Recovery Results for DHBIs in Tap Water**

| recovery results of HQ in local tap water containing CC and RS at HBPE | | | | |
|---|---|---|---|---|
| sample no. | tap water containing CC and RS (mM) | HQ added (mM) | HQ found (mM) | Recovery (%) |
| 1 | 1.0 | 1.0 | 0.9 | 90 |
| 2 | 1.0 | 2.0 | 1.8 | 90 |
| 3 | 1.0 | 3.0 | 2.8 | 93 |
| recovery results of CC in local tap water containing HQ and RS at HBPE | | | | |
| sample no. | tap water containing HQ and RS (mM) | CC added (mM) | CC found (mM) | Recovery (%) |
| 1 | 1.0 | 1.0 | 1.1 | 110 |
| 2 | 1.0 | 2.0 | 2.1 | 105 |
| 3 | 1.0 | 3.0 | 3.2 | 106 |
| recovery results of RS in local tap water containing HQ and CC at HBPE | | | | |
| sample no. | tap water containing HQ and CC (mM) | RS added (mM) | RS found (mM) | recovery (%) |
| 1 | 1.0 | 1.0 | 1.2 | 120 |
| 2 | 1.0 | 2.0 | 2.3 | 115 |
| 3 | 1.0 | 3.0 | 3.1 | 103 |
| recovery results of HQ in local tap water containing CC and RS at GLY-HB | | | | |
| sample no. | tap water containing CC and RS (mM) | HQ added (mM) | HQ found (mM) | recovery (%) |
| 1 | 1.0 | 1.0 | 1.1 | 110 |
| 2 | 1.0 | 2.0 | 2.1 | 105 |
| 3 | 1.0 | 3.0 | 3.2 | 106 |
| recovery results of CC in local tap water containing HQ and RS at GLY-HB | | | | |
| sample no. | tap water containing HQ and RS (mM) | CC added (mM) | CC found (mM) | recovery (%) |
| 1 | 1.0 | 1.0 | 1.1 | 110 |
| 2 | 1.0 | 2.0 | 2.2 | 110 |
| 3 | 1.0 | 3.0 | 3.2 | 106 |
| recovery results of RS in local tap water containing HQ and CC at GLY-HB | | | | |
| sample no. | tap water containing HQ and CC (mM) | RS added (mM) | RS found (mM) | recovery (%) |
| 1 | 1.0 | 1.0 | 1.0 | 100 |
| 2 | 1.0 | 2.0 | 2.1 | 105 |
| 3 | 1.0 | 3.0 | 3.2 | 106 |
| recovery results of HQ in local tap water containing CC and RS at ASA-HB | | | | |
| sample no. | tap water containing CC and RS (mM) | HQ added (mM) | HQ found (mM) | recovery (%) |
| 1 | 1.0 | 1.0 | 0.9 | 90 |
| 2 | 1.0 | 2.0 | 1.8 | 90 |
| 3 | 1.0 | 3.0 | 2.8 | 93 |
| recovery results of CC in local tap water containing HQ and RS at ASA-HB | | | | |
| sample no. | tap water containing HQ and RS (mM) | CC added (mM) | CC found (mM) | recovery (%) |
| 1 | 1.0 | 1.0 | 1.2 | 120 |
| 2 | 1.0 | 2.0 | 2.2 | 110 |
| 3 | 1.0 | 3.0 | 3.1 | 103 |
| recovery results of RS in local tap water containing HQ and CC at ASA-HB | | | | |
| sample no. | tap water containing HQ and CC (mM) | RS added (mM) | RS found (mM) | recovery (%) |
| 1 | 1.0 | 1.0 | 1.2 | 120 |
| 2 | 1.0 | 2.0 | 2.2 | 110 |
| 3 | 1.0 | 3.0 | 3.0 | 100 |

HB and ASA-HB successfully gave satisfactory results and could detect and quantify DHBIs explicitly from their aqueous mixture. HQ, CC, and RS showed reversible, quasi-reversible, and irreversible behavior, respectively, on all electrodes by CV. The anodic peak current versus the concentration of HQ, CC, and RS showed a linear relationship, and the electrochemical process was diffusion controlled. DPV worked on more effectual detection and quantification of DHBIs. By using DPV, three peaks of three isomers were detected effectively in their binary and ternary mixtures. All electrodes could detect DHBIs simultaneously with high sensitivity and a considerable detection limit. HBPE is at least 2800 times cheaper and that for GLY-HB or ASA-HB electrode is 2000 times cheaper than conventional commercial GCE.

## ■ ASSOCIATED CONTENT

### Supporting Information

The Supporting Information is available free of charge at https://pubs.acs.org/doi/10.1021/acsomega.2c03651.

CVs of HQ in PBS (pH 6.8) at different scan rates (Figure S1), CVs of HQ at different concentrations in PBS (pH 6.8) at 50 $mVs^{-1}$ (Figure S2), CVs of CC in PBS (pH 6.8) at different scan rates (Figure S3), CVs of CC at different concentrations in PBS (pH 6.8) at 50 $mVs^{-1}$ (Figure S4), CVs of RS in PBS (pH 6.8) at different scan rates (Figure S5), CVs of RS at different concentrations in PBS (pH 6.8) at 50 $mVs^{-1}$ (Figure S6) (PDF)

## ■ AUTHOR INFORMATION


### Corresponding Author

**Nusrat T. Tonu** − *Department of Chemistry, Khulna University of Engineering and Technology, Khulna 9203, Bangladesh; Chemistry Discipline, Khulna University, Khulna 9208, Bangladesh;* orcid.org/0000-0001-5672-3548; Email: nusrattazeen@ku.ac.bd

### Authors

**Md. Muzahedul I. Khan** − *Department of Chemistry, Khulna University of Engineering and Technology, Khulna 9203, Bangladesh*

**Mohammad A. Yousuf** − *Department of Chemistry, Khulna University of Engineering and Technology, Khulna 9203, Bangladesh*

**Parbhej Ahamed** − *Department of Chemistry, Khulna University of Engineering and Technology, Khulna 9203, Bangladesh*

**Mohammad Alauddin** − *Department of Theoretical and Computational Chemistry, University of Dhaka, Dhaka 1000, Bangladesh*

Complete contact information is available at: https://pubs.acs.org/10.1021/acsomega.2c03651


### Notes

The authors declare no competing financial interest.

## ■ ACKNOWLEDGMENTS

This work was supported by Committee for Advanced Studies and Research (Fund ID: KUET/CASR-43/22), Khulna University of Engineering and Technology, Khulna, Bangladesh.

## ■ REFERENCES

(1) Ganesh, P. S.; Shimoga, G.; Lee, S.-H.; Kim, S.-Y.; Ebenso, E. E. Simultaneous electrochemical sensing of dihydroxy benzene isomers at cost-effective allura red polymeric film modified glassy carbon electrode. *J. Anal. Sci. Technol.* **2021**, *12* (1), 1−14.

(2) Tonu, N. T.; Yousuf, A. Simultaneous Electrochemical Determination of Dihydroxybenzene Isomers at 1-Butyl-3-Methyl-imidazolium Hexafluorophosphate Modified Pencil Graphite Electrode. *J. Mater. Environ. Sci.* **2021**, *12* (3), 384−397.
(3) Manjunatha, J. G. Poly (Adenine) Modified Graphene-Based Voltammetric Sensor for the Electrochemical Determination of Catechol, Hydroquinone and Resorcinol. *Open Chem. Eng. J.* **2020**, *14* (1), 52−62.
(4) Tonu, N. T.; Yousuf, M. A. Low Cost Electrochemical Sensor for Simultaneous Detection and Estimation of Dihydroxybenzene Isomers. *Port. Electrochim. Acta* **2022**, *39*, 59−71.
(5) Ahammad, A. J. S.; Akter, T.; Mamun, A. A.; Islam, T.; Hasan, Md. M.; Mamun, M. A.; Faraezi, S.; Monira, F. Z.; Saha, J. K. Cost-Effective Electrochemical Sensor Based on Carbon Nanotube Modified-Pencil Electrode for the Simultaneous Determination of Hydroquinone and Catechol. *J. Electrochem. Soc.* **2018**, *165* (9), B390−B397.
(6) Bukhari, S. A. B.; Nasir, H.; Pan, L.; Tasawar, M.; Sohail, M.; Shahbaz, M.; Gul, F.; Sitara, E. Supramolecular assemblies of carbon nanocoils and tetraphenylporphyrin derivatives for sensing of catechol and hydroquinone in aqueous solution. *Sci. Rep.* **2021**, *11* (1), 5044.
(7) Huang, L.; Cao, Y.; Diao, D. Electrochemical activation of graphene sheets embedded carbon films for high sensitivity simultaneous determination of hydroquinone, catechol and resorcinol. *Sens. and Actuators B Chem.* **2020**, *305*, 127495.
(8) Gu, C. C.; Li, X. P.; Liu, H. Y. Simultaneous Determination of Hydroquinone, and Catechol Using a Multi-Walled Carbon Nanotube/GC Electrode Modified by Electrodeposition of Carbon Nanodots. *JNanoR.* **2018**, *54*, 42−53.
(9) Bu, C.; Liu, X.; Zhang, Y.; Li, L.; Zhou, X.; Lu, X. A sensor based on the carbon nanotubes-ionic liquid composite for simultaneous determination of hydroquinone and catechol. *Colloids Surf., B* **2011**, *88* (1), 292−296.
(10) Wang, C.; Yuan, R.; Chai, Y.; Hu, F. Simultaneous determination of hydroquinone, catechol, resorcinol and nitrite using gold nanoparticles loaded on poly-3-amino-5-mercapto-1,2,4-triazole-MWNTs film modified electrode. *Anal. Methods* **2012**, *4* (6), 1626−1628.
(11) Deng, D.-H.; Li, S.-J.; Zhang, M.-J.; Liu, X.-N.; Zhao, M.-M.; Liu, L. Anti-adsorption properties of gold nanoparticle/sulfonated graphene composites for simultaneous determination of dihydroxybenzene isomers. *Anal. Methods.* **2013**, *5* (10), 2536−2542.
(12) Zhao, D.-M.; Zhang, X.-H.; Feng, L.-J.; Jia, L.; Wang, S.-F. Simultaneous determination of hydroquinone and catechol at PASA/MWNTs composite film modified glassy carbon electrode. *Colloids Surf., B* **2009**, *74* (1), 317−321.
(13) Kong, F.-Y.; Li, R.-F.; Yao, L.; Wang, Z.-X.; Li, H.-Y.; Lv, W.-X.; Wang, W. Voltammetric simultaneous determination of catechol and hydroquinone using a glassy carbon electrode modified with a ternary hybrid material composed of reduced graphene oxide, magnetite nanoparticles and gold nanoparticles. *Microchim Acta.* **2019**, *186* (3), 1−8.
(14) Yin, H.; Zhang, Q.; Zhou, Y.; Ma, Q.; liu, T.; Zhu, L.; Ai, S. Electrochemical behavior of catechol, resorcinol and hydroquinone at graphene-chitosan composite film modified glassy carbon electrode and their simultaneous determination in water samples. *Electrochim. Acta* **2011**, *56* (6), 2748−2753.
(15) Hassan, K. M.; Hathoot, A. A.; Abo oura, M. F.; Azzem, M. A. Simultaneous and selective electrochemical determination of hydroquinone, catechol and resorcinol at poly (1,5-diaminonaphthalene)/glassy carbon-modified electrode in different media. *RSC Adv.* **2018**, *8* (12), 6346−6355.
(16) Wang, L.; Huang, P.; Wang, H.; Bai, J.; Zhang, L.; Zhao, Y. Covalent Modification of Glassy Carbon Electrode with Aspartic Acid for Simultaneous Determination of Hydroquinone and Catechol. *Ann. Chim.* **2007**, *97*, 395−404.
(17) Tang, L.; Zhou, Y.; Zeng, G.; Li, Z.; Liu, Y.; Zhang, Y.; Chen, G.; Yang, G.; Lei, X.; Wu, M. A tyrosinase biosensor based on ordered mesoporous carbon-Au/l-lysine/Au nanoparticles for simultaneous determination of hydroquinone and catechol. *Analyst.* **2013**, *138* (12), 3552−3560.
(18) Alshahrani, L. A.; Miao, L.; Zhang, Y.; Cheng, S.; Sathishkumar, P.; Saravanakumar, B.; Nan, J.; Gu, F. L. 3D-Flower-Like Copper Sulfide Nanoflake-Decorated Carbon Nanofragments-Modified Glassy Carbon Electrodes for Simultaneous Electrocatalytic Sensing of Co-existing Hydroquinone and Catechol. *Sensors.* **2019**, *19* (10), 2289.
(19) Liu, H.-Y.; Zhu, L.-L.; Huang, Z.-H.; Qiu, Y.-B.; Xu, H.-X.; Wen, J.-J.; Xiong, W.-W.; Li, L.-H.; Gu, C.-C. Simultaneous Detection of Hydroquinone, Catechol and Resorcinol by an Electrochemical Sensor Based on Ammoniated-Phosphate Buffer Solution Activated Glassy Carbon Electrode. *Chin. J. Anal. Chem.* **2019**, *47* (9), e19113−e19120.
(20) Goulart, L. A.; Gonçalves, R.; Correa, A. A.; Pereira, E. C.; Mascaro, L. H. Synergic effect of silver nanoparticles and carbon nanotubes on the simultaneous voltammetric determination of hydroquinone, catechol, bisphenol A and phenol. *Microchim. Acta.* **2017**, *185* (1), 1−9.
(21) Hossain, Md. U.; Rahman, Md. T.; Ehsan, Md. Q. Simultaneous Detection and Estimation of Catechol, Hydroquinone, and Resorcinol in Binary and Ternary Mixtures Using Electrochemical Techniques. *Int. J. Anal. Chem.* **2015**, *2015*, 1−8.
(22) Zhang, M.; Ge, C.; Jin, Y.; Hu, L.; Mo, H.; Li, X.; Zhang, H. Sensitive and Simultaneous Determination of Hydroquinone and Catechol in Water Using an Anodized Glassy Carbon Electrode with Polymerized 2-(Phenylazo) Chromotropic Acid. *J. Chem.* **2019**, *2019*, 1−10.
(23) Edris, N. M. M. A.; Abdullah, J.; Kamaruzaman, S.; Sulaiman, Y. Voltammetric determination of hydroquinone, catechol, and resorcinol by using a glassy carbon electrode modified with electrochemically reduced graphene oxide-poly(Eriochrome black T) and gold nanoparticles. *Microchim. Acta.* **2019**, *186* (4), 1−9.
(24) Yang, P.; Zhu, Q.; Chen, Y.; Wang, F. Simultaneous determination of hydroquinone and catechol using poly(p-amino-benzoic acid) modified glassy carbon electrode. *J. Appl. Polym. Sci.* **2009**, *113* (5), 2881−2886.
(25) Singh, R. P. A catechol biosensor based on a gold nanoparticles encapsulated-dendrimer. *Analyst.* **2011**, *136* (6), 1216−1221.
(26) Huang, R.; Chen, S.; Yu, J.; Jiang, X. Self-assembled Ti3C2/MWCNTs nanocomposites modified glassy carbon electrode for electrochemical simultaneous detection of hydroquinone and catechol. *Ecotox. Environ. Safe.* **2019**, *184*, 109619.
(27) Piña, S.; Candia-Onfray, C.; Hassan, N.; Jara-Ulloa, P.; Contreras, D.; Salazar, R. Glassy Carbon Electrode Modified with C/Au Nanostructured Materials for Simultaneous Determination of Hydroquinone and Catechol in Water Matrices. *Chemosensors.* **2021**, *9* (5), 88.
(28) Palanisamy, S.; Ramaraj, S. K.; Chen, S.-M.; Velusamy, V.; Yang, T. C. K.; Chen, T.-W. Voltammetric determination of catechol based on a glassy carbon electrode modified with a composite consisting of graphene oxide and polymelamine. *Microchim. Acta.* **2017**, *184* (4), 1051−1057.
(29) Liu, W.; Wu, L.; Zhang, X.; Chen, J. Simultaneous Electrochemical Determination of Hydroquinone, Catechol and Resorcinol at Nitrogen Doped Porous Carbon Nanopolyhedrons-multiwall Carbon Nanotubes Hybrid Materials Modified Glassy Carbon Electrode. *Bull. Korean Chem. Soc.* **2014**, *35* (1), 204−210.
(30) Li, X.; Xu, G.; Jiang, X.; Tao, J. Highly Sensitive and Simultaneous Determination of Hydroquinone and Catechol at Thionine/Graphene Oxide Modified Glassy Carbon Electrodes. *J. Electrochem. Soc.* **2014**, *161* (9), H464−H468.
(31) Liu, X.; Ding, Z.; He, Y.; Xue, Z.; Zhao, X.; Lu, X. Electrochemical behavior of hydroquinone at multi-walled carbon nanotubes and ionic liquid composite film modified electrode. *Colloid Surf., B* **2010**, *79* (1), 27−32.
(32) Wang, X.; Xi, M.; Guo, M.; Sheng, F.; Xiao, G.; Wu, S.; Uchiyama, S.; Matsuura, H. An electrochemically aminated glassy


https://doi.org/10.1021/acsomega.2c03651
ACS Omega 2022, 7, 29391−29405

carbon electrode for simultaneous determination of hydroquinone and catechol. *Analyst.* **2016**, *141* (3), 1077−1082.
(33) Umasankar, Y.; Periasamy, A. P.; Chen, S.-M. Electrocatalysis and simultaneous determination of catechol and quinol by poly-(malachite green) coated multiwalled carbon nanotube film. *Anal. Biochem.* **2011**, *411* (1), 71−79.
(34) Shen, Y.; Rao, D.; Sheng, Q.; Zheng, J. Simultaneous voltammetric determination of hydroquinone and catechol by using a glassy carbon electrode modified with carboxy-functionalized carbon nanotubes in a chitosan matrix and decorated with gold nanoparticles. *Microchim. Acta.* **2017**, *184* (9), 3591−3601.
(35) Khalifa, Z.; Hassan, K.; Abo Oura, M. F.; Hathoot, A.; Azzem, M. A. Individual and Simultaneous Voltammetric Determination of Ultra-Trace Environmental Contaminant Dihydroxybenzene Isomers Based on a Composite Electrode Sandwich-like Structure. *ACS Omega.* **2020**, *5* (30), 18950−18957.
(36) Chetankumar, K.; Swamy, B. E. K.; Sharma, S. C. Electrochemical preparation of poly (direct yellow 11) modified pencil graphite electrode sensor for catechol and hydroquinone in presence of resorcinol: A voltammetric study. *Microchem J.* **2020**, *156*, 104979.
(37) Buleandra, M.; Rabinca, A. A.; Badea, I. A.; Balan, A.; Stamatin, I.; Mihailciuc, C.; Ciucu, A. A. Voltammetric determination of dihydroxybenzene isomers using a disposable pencil graphite electrode modified with cobalt-phthalocyanine. *Microchim. Acta.* **2017**, *184* (5), 1481−1488.
(38) Ghanem, M. A. Electrocatalytic activity and simultaneous determination of catechol and hydroquinone at mesoporous platinum electrode. *Electrochem. Commun.* **2007**, *9* (10), 2501−2506.
(39) Ganesh, P. S.; Swamy, B. E. K.; Fayemi, O. E.; Sherif, E.-S. M.; Ebenso, E. E. Poly(crystal violet) modified pencil graphite electrode sensor for the electroanalysis of catechol in the presence of hydroquinone. *Sens. Bio-Sens. Res.* **2018**, *20*, 47−54.
(40) Sá, A. C. de; Barbosa, S. C.; Raymundo-Pereira, P. A.; Wilson, D.; Shimizu, F. M.; Raposo, M.; Oliveira, O. N. Flexible Carbon Electrodes for Electrochemical Detection of Bisphenol-A, Hydroquinone and Catechol in Water Samples. *Chemosensors.* **2020**, *8* (4), 103.
(41) Huang, L.; Cao, Y.; Diao, D. Electrochemical activation of graphene sheets embedded carbon films for high sensitivity simultaneous determination of hydroquinone, catechol and resorcinol. *Sens and Actuators B* **2020**, *305*, 127495.
(42) Ma, L.; Zhao, G.-C. Simultaneous Determination of Hydroquinone, Catechol and Resorcinol at Graphene Doped Carbon Ionic Liquid Electrode. *Int. J. Electrochem.* **2012**, *2012*, 1−8.
(43) Hu, S.; Wang, Y.; Wang, X.; Xu, L.; Xiang, J.; Sun, W. Electrochemical detection of hydroquinone with a gold nanoparticle and graphene modified carbon ionic liquid electrode. *Sens and Actuators B* **2012**, *168*, 27−33.
(44) Nambiar, S. R.; Aneesh, P. K.; Rao, T. P. Ultrasensitive voltammetric determination of catechol at a gold atomic cluster/poly (3,4-ethylenedioxythiophene) nanocomposite electrode. *Analyst.* **2013**, *138* (17), 5031.
(45) Sathisha, A.; Swamy, B. E. K. Electrosensitive Determination of Paracetamol Using a Poly (glycine) Film Coated Graphite Pencil Electrode: A Cyclic Voltammetric Study. *Anal. Bioanal. Electrochem.* **2015**, *7* (1), 12−21.
(46) Kariuki, J.; Ervin, E.; Olafson, C. Development of a Novel, Low-Cost, Disposable Wooden Pencil Graphite Electrode for Use in the Determination of Antioxidants and Other Biological Compounds. *Sensors.* **2015**, *15* (8), 18887−18900.
(47) Sengiz, C.; Congur, G.; Erdem, A. Development of Ionic Liquid Modified Disposable Graphite Electrodes for Label-Free Electrochemical Detection of DNA Hybridization Related to Microcystis spp. *Sensors.* **2015**, *15* (9), 22737−22749.
(48) Özcan, L.; Sahin, M.; Sahin, Y. Electrochemical Preparation of a Molecularly Imprinted Polypyrrole-modified Pencil Graphite Electrode for Determination of Ascorbic Acid. *Sensors.* **2008**, *8* (9), 5792−5805.
(49) Alipour, E.; Majidi, M. R.; Saadatirad, A.; mahdi Golabi, S.; Alizadeh, A. M. Simultaneous determination of dopamine and uric acid in biological samples on the pretreated pencil graphite electrode. *Electrochim. Acta* **2013**, *91*, 36−42.
(50) Gong, Z. Q.; Sujari, A. N. A.; Ab Ghani, S. Electrochemical fabrication, characterization and application of carboxylic multi-walled carbon nanotube modified composite pencil graphite electrodes. *Electrochim. Acta* **2012**, *65*, 257−265.
(51) Chehreh Chelgani, S.; Rudolph, M.; Kratzsch, R.; Sandmann, D.; Gutzmer, J. A review of graphite beneficiation techniques. *Miner. Process. Extr. Metall. Rev.* **2016**, *37* (1), 58−68.
(52) Zhang, Y.; Xu, J.; Long, Y.; Tao, L.; Ding, M.; Jia, C. Defect chemistry on electrode materials for electrochemical energy storage and conversion. *ChemNanoMater.* **2020**, *6* (11), 1589−1600.
(53) Wei, P.; Shen, J.; Wu, K.; Yang, N. Defect-dependent electrochemistry of exfoliated graphene layers. *Carbon* **2019**, *154*, 125−131.
(54) Kudur Jayaprakash, G.; Casillas, N.; Astudillo-Sánchez, P. D.; Flores-Moreno, R. Role of defects on regioselectivity of nano pristine graphene. *J. Phys. Chem. A* **2016**, *120* (45), 9101−9108.
(55) Nie, Z.; Ong, S.; Hussey, D. S.; LaManna, J. M.; Jacobson, D. L.; Koenig, G. M. Probing transport limitations in thick sintered battery electrodes with neutron imaging. *Mol. Syst. Des. Eng.* **2020**, *5* (1), 245−256.
(56) Hou, C.; Hou, J.; Zhang, H.; Ma, Y.; He, X.; Geng, W.; Zhang, Q. Facile synthesis of LiMn0. 75Fe0. 25PO4/C nanocomposite cathode materials of lithium-ion batteries through microwave sintering. *Eng. Sci.* **2020**, *11* (4), 36−43.
(57) Khullar, P.; Badilla, J. V.; Kelly, R. G. The Use of a Sintered Ag/AgCl Electrode as Both Reference and Counter Electrode for Electrochemical Measurements in Thin Film Electrolytes. *ECS Electrochem. Lett.* **2015**, *4* (10), C31.
(58) Robinson, J. P.; Ruppert, J. J.; Dong, H.; Koenig, G. M. Sintered electrode full cells for high energy density lithium-ion batteries. *J. Appl. Electrochem.* **2018**, *48* (11), 1297−1304.
(59) Kudur Jayaprakash, G.; Swamy, B.E. K.; Casillas, N.; Flores-Moreno, R. Analytical Fukui and cyclic voltammetric studies on ferrocene modified carbon electrodes and effect of Triton X-100 by immobilization method. *Electrochim. Acta* **2017**, *258*, 1025−1034.
(60) Jayaprakash, G. K.; Flores-Moreno, R. Quantum chemical study of Triton X-100 modified graphene surface. *Electrochim. Acta* **2017**, *248*, 225−231.
(61) Kudur Jayaprakash, G.; Swamy, B.E. K.; Sanchez, J. P. M.; Li, X.; Sharma, S.C.; Lee, S.-L. Electrochemical and quantum chemical studies of cetylpyridinium bromide modified carbon electrode interface for sensor applications. *J. Mol. Liq.* **2020**, *315*, 113719.
(62) Jayaprakash, G. K.; Kumara Swamy, B.E.; Rajendrachari, S.; Sharma, S.C.; Flores-Moreno, R. Dual descriptor analysis of cetylpyridinium modified carbon paste electrodes for ascorbic acid sensing applications. *J. Mol. Liq.* **2021**, *334*, 116348.
(63) Hassan, K. M.; Hathoot, A. A.; Azzem, M. A. Simultaneous and selective electrochemical determination of hydroquinone, catechol and resorcinol at poly (1, 5-diaminonaphthalene)/glassy carbon-modified electrode in different media. *RSC advances.* **2018**, *8* (12), 6346−6355.
(64) Liu, L.; Ma, Z.; Zhu, X.; Zeng, R.; Tie, S.; Nan, J. Electrochemical behaviour and simultaneous determination of catechol, resorcinol, and hydroquinone using thermally reduced carbon nano-fragment modified glassy carbon electrode. *Analytical Methods.* **2016**, *8* (3), 605−613.
(65) Li, M.; Ni, F.; Wang, Y.; Xu, S.; Zhang, D.; Chen, S.; Wang, L. Sensitive and facile determination of catechol and hydroquinone simultaneously under coexistence of resorcinol with a Zn/Al layered double hydroxide film modified glassy carbon electrode. *Electroanalysis: An International Journal Devoted to Fundamental and Practical Aspects of Electroanalysis.* **2009**, *21* (13), 1521−1526.


https://doi.org/10.1021/acsomega.2c03651
*ACS Omega* 2022, 7, 29391−29405